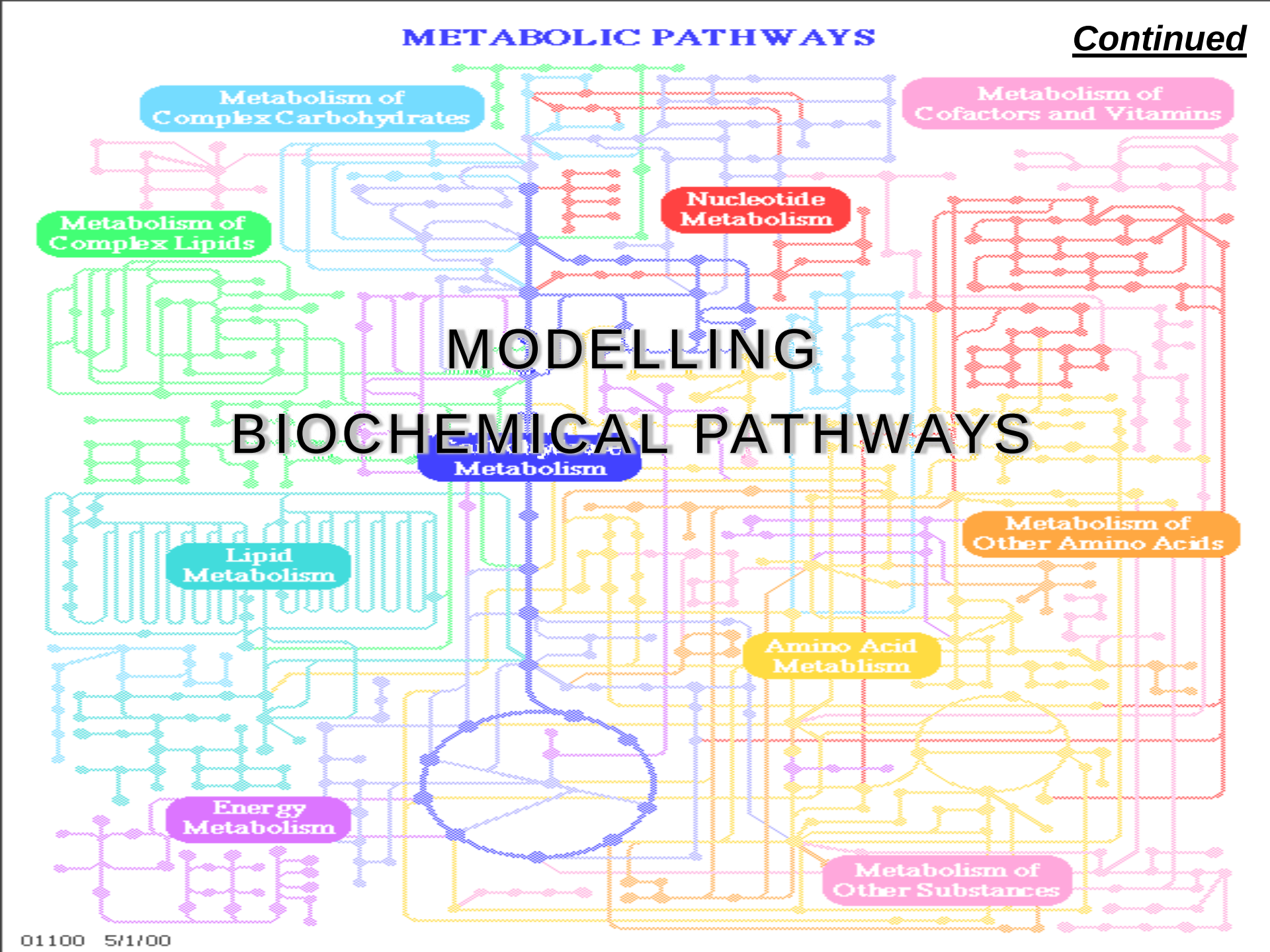
METABOLIC PATHWAYS
Continued
Metabolism of Complex Carbohydrates
Metabolism of Cofactors and Vitamins
Metabolism of Complex Lipids
Nucleotide Metabolism
MODELLING
BIOCHEMICAL PATHWAYS
Metabolism
Metabolism of Other Amino Acids
Lipid Metabolism
Amino Acid Metablism
Energy Metabolism
Metabolism of Other Substances
01100 5/1/00

HOW DO PATTERNS OF REGULATION AFFECT FUNCTIONAL DYNAMICS ?

Model existing pathways based on
biochemical & genetic information
Tryptophan biosynthetic pathway in bacteria

Study the dynamics of simple pathways having different structural designs/arrangements of feedback regulation

Study the dynamic behaviour of these pathways under realistic changes (mutations) and stochastic variation in reaction rates, or concentration of substrates

Biosynthesis of Aromatic Amino Acids

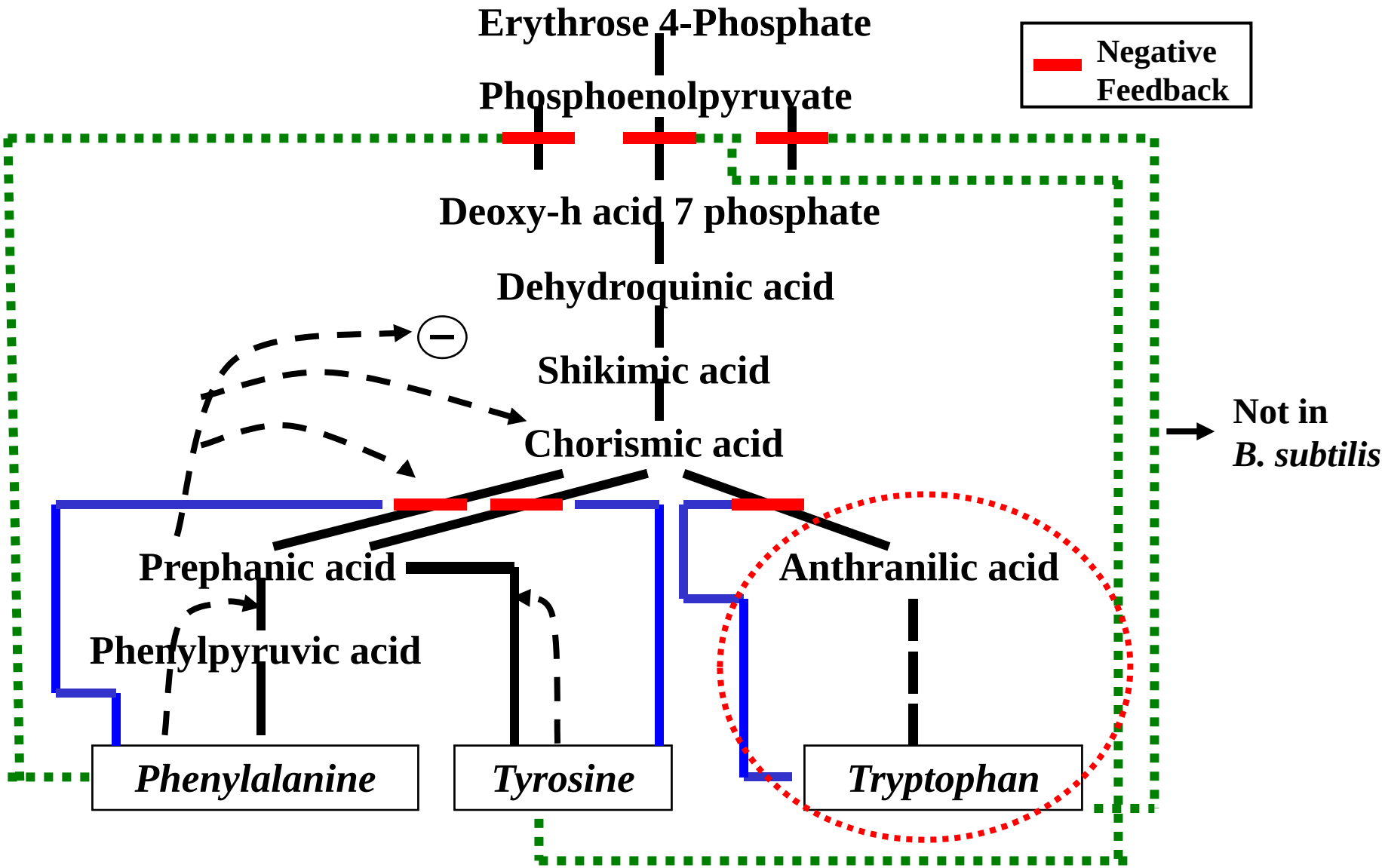

Variation in regulation of the same pathway in different microorganisms

Dual nested feedback in Tryptophan biosynthetic pathway

GENETIC — **Two levels of control** — **METABOLIC**

Gene repression through Trp repressor

Enzyme inhibition by end product

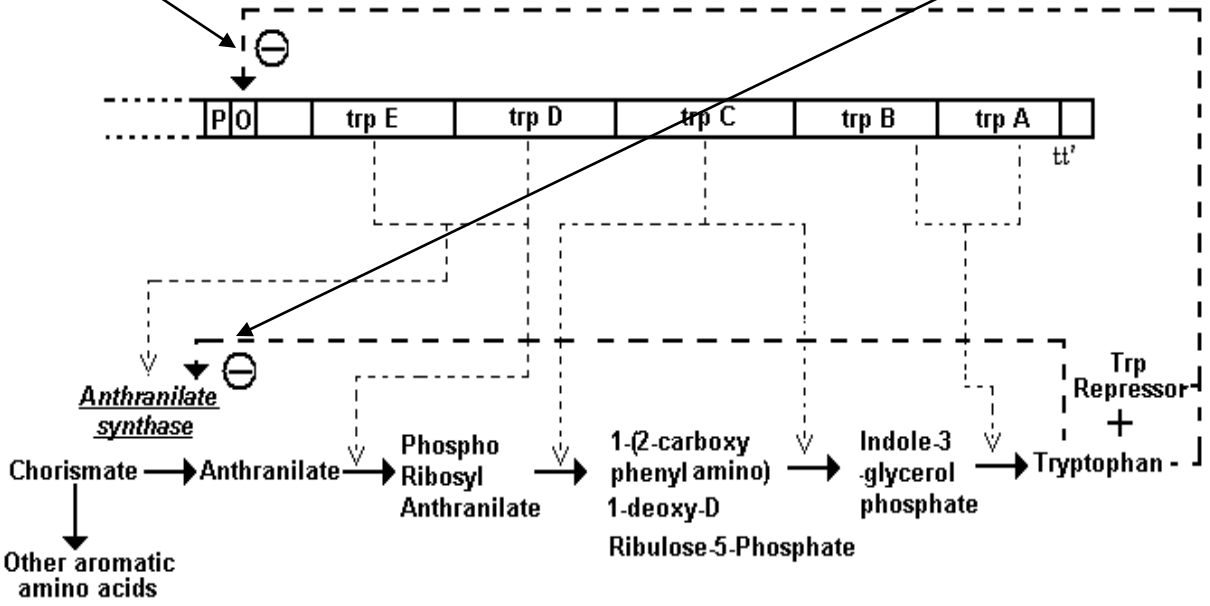

Tryptophan Biosynthetic Pathway Model

The time variation of concentrations of A,B, and C are -

$$\frac{dA}{dt} = \frac{r}{1+r}\frac{K_m D K_d}{K_d + (1+r)C} + \frac{K_m D}{1+r} - K_1 A$$

$$\frac{K_R^{\,n}}{K_R^{\,n} + (1+r)C^n}$$

$$\frac{dB}{dt} = K_e A - K_2 B$$

$$\frac{dC}{dt} = K_P \frac{K_I^{\,2} B}{K_I^{\,2} + C^2} - K_D C - \frac{V_{max} C}{K_G + C}$$

V_{max}

A ***trp*** **mRNA**
B **Enzyme (*Asase*)**
C **Tryptophan**

12 parameters

The dimensionless form of the equations are

7 parameters

$$\frac{dX}{dt} = \left[\frac{r}{1+r}\right]\frac{1}{1+(1+r)\,Z} + \frac{1}{(1+r)} - a_1 X$$

$$\frac{dY}{dt} = X - a_2 Y$$

$$\frac{dZ}{dt} = \frac{Y}{1+\beta Z^2} - a_3 Z - g\,\frac{Z}{K'+Z}$$

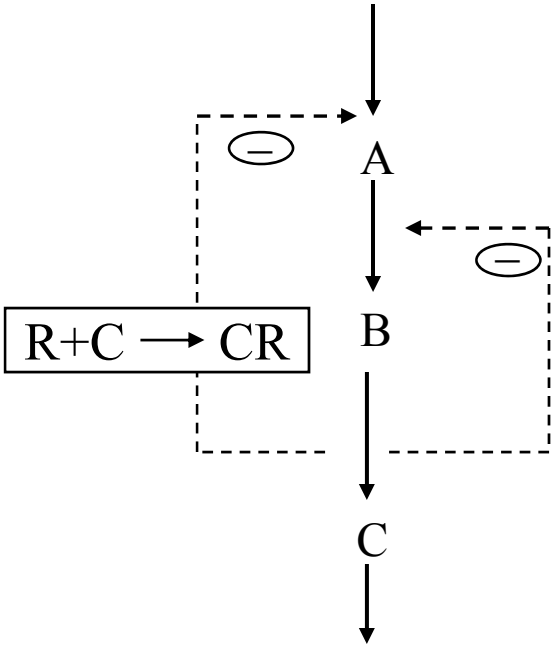

a1, a2, a3 — **degradation rates of A, B and C**

r and β — **gene repression and enzyme inhibition strengths**

g and K' — **tryptophan utilization in the cell**

This is the basic model for tryptophan biosynthetic pathway in *E.coli*

This structure of regulation is not universal and different organisms show significant variability

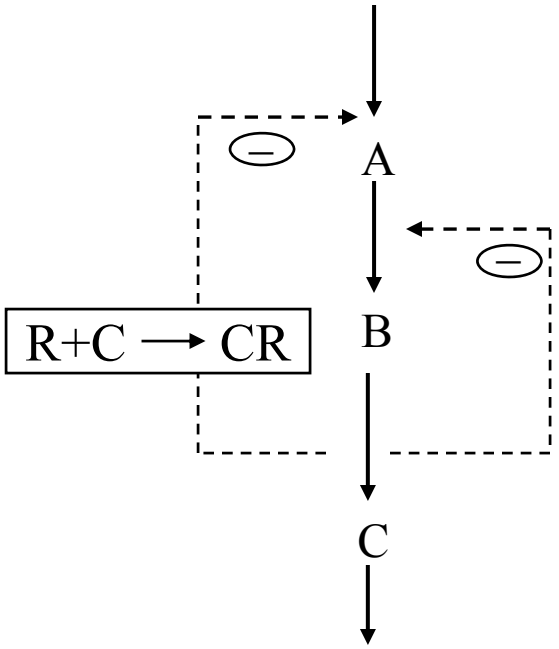

A ⟶ mRNA

B ⟶ Enzymes

C ⟶ tryptophan

R ⟶ inactive repressor

CR ⟶ active repressor

Pathways with different structural designs show distinct functional dynamics and degrees of robustness to environmental noise

Three major regulatory schemes -

Dual control - endproduct inhibition of enzyme activity, and repressor-mediated repression of transcription of the operon.
Bacteria *E.coli* and *Salmonella typhimurium*

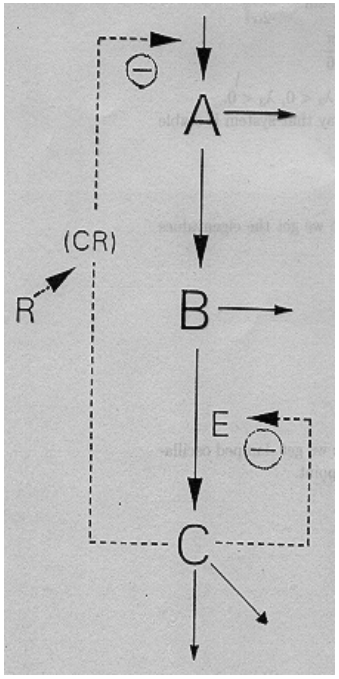

Control by repressor-mediated repression of transcription alone.
Rhizobium leguminosarum
(2 genes)

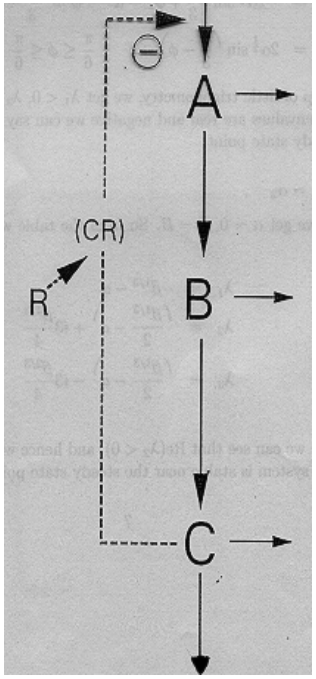

Control by end product inhibition of enzyme activity alone.
Chromobacterium violecium,
Loose-repressing mutants of *E.coli*.

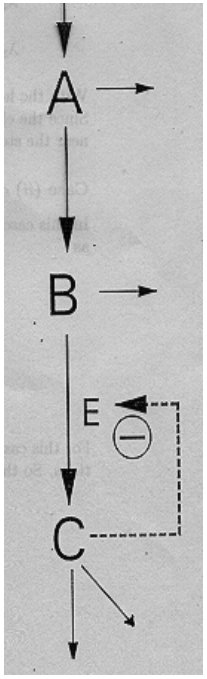

Single Negative Feedback Pathway: Repressor mediated repression

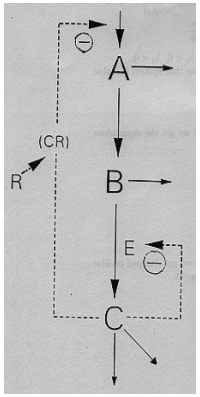

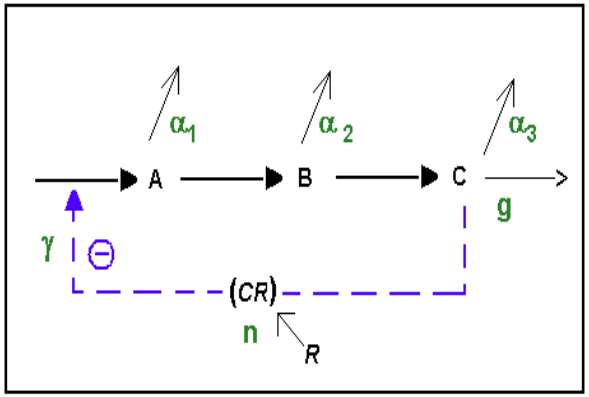

$$\frac{dx}{dt}=\left(\frac{\gamma}{1+\gamma}\right)\frac{1}{1+(1+\gamma)z^{n}}-\alpha_1 x+\left(\frac{1}{1+\gamma}\right)$$

$$\frac{dy}{dt}=x-\alpha_2 y$$

$$\frac{dz}{dt}=y-\alpha_3 z-g$$

Two Negative Feedback Pathway: Repressor-mediated repression and enzyme inhibition

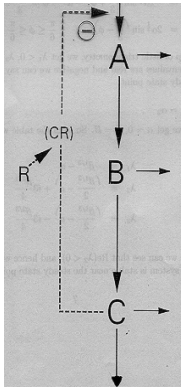

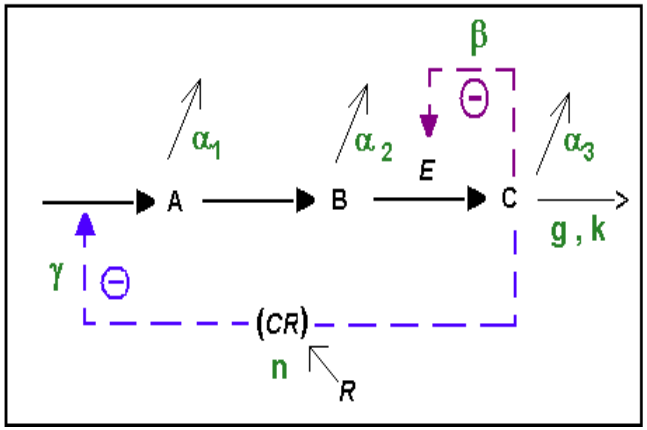

$$\frac{dx}{dt}=\left(\frac{\gamma}{1+\gamma}\right)\frac{1}{1+(1+\gamma)z^{n}}-\alpha_1 x+\left(\frac{1}{1+\gamma}\right)$$

$$\frac{dy}{dt}=x-\alpha_2 y$$

$$\frac{dz}{dt}=\frac{y}{1+\beta z^{2}}-\alpha_3 z-g\frac{z}{k+z}$$

- x ,y, z are scaled concentrations of A, B, and C
- a is the strength of repression of C on A
- n is the co-operativity of repressor-mediated repression
- g is related to the utilisation of end-product in cellular processes
- α_1, α_2 and α_3 are degradation rates of x, y and z

The additional parameters are:

β strength of enzyme inhibition of C on the enzyme E

k related to utilization of end-product in cellular processes

Experimental parameter values for the Tryptophan biosynthetic pathway in *E.coli*

Parameter	Units	Magnitude
D	Operons/cell	1.3
K_m	mRNA/operon/sec	0.07
K_e	Emzyme/mRNA/sec	0.28
K_1, K_2	1/sec	0.016, 0.0002
K_R	Molar	$1/1.73 \times 10^{-4}$
K_I	Molar	10^{-4} (normal operon)
K_I	Molar	10^{-3} (feedback resistant)
K_G	Molar	10^{-6}
K_D	1/sec	0.0002
K_P	Moles end-prod/ enzyme molec/cell litres/cell	10^{-8}

a1 = 1

a2 = 0.01

a3 = 0.01

g = 4

r = 10

Gene repression function

$$F(z) = (r/(1+r))[1/(1+(1+r)z^n)]$$

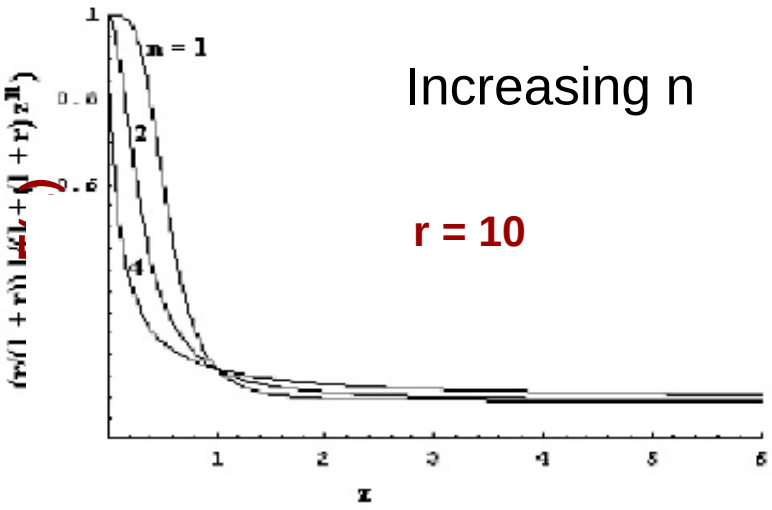

Increasing n

r = 10

Switch-like repression for increasing "n" and "r"

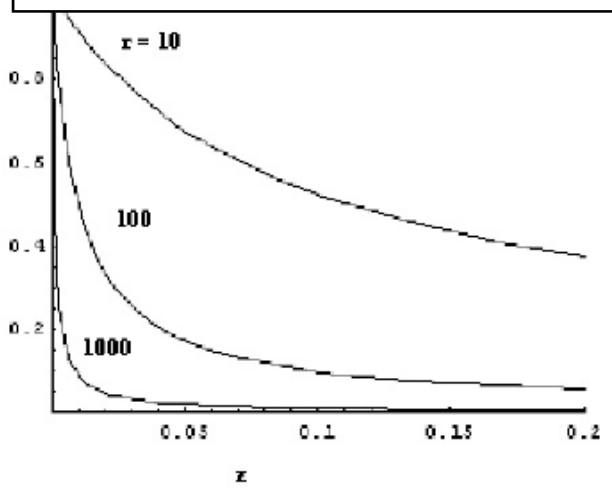

Enzyme inhibition function

$$G(y,z) = y / (1+ bz^2)$$

Increasing y

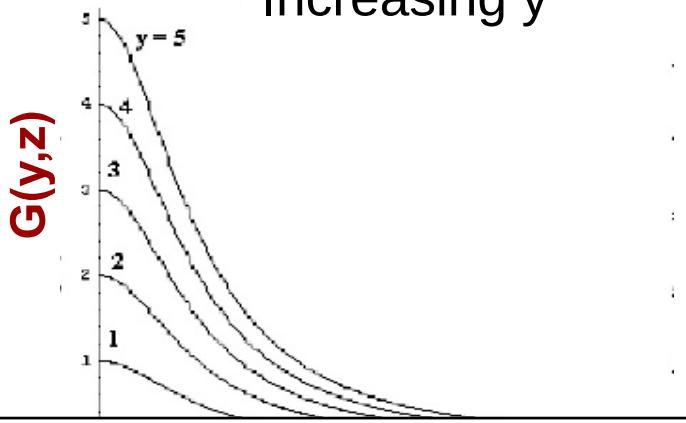

Stronger inhibition for increasing enzyme conc. & strength of inhibition

decreasing b

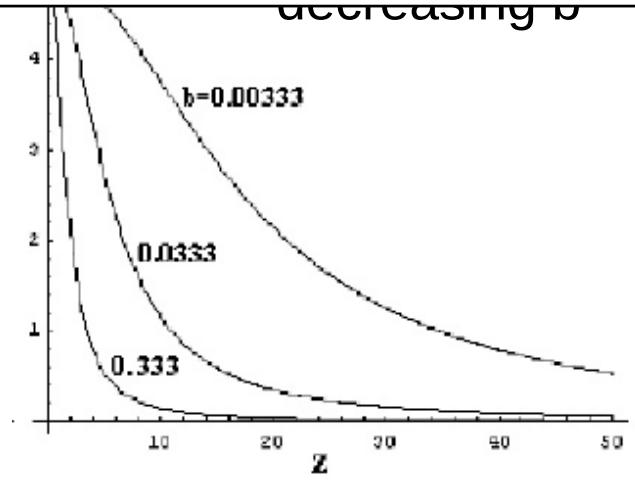

a1 = 1, a2 =.02,
a3 = .01, g = 4,
β ,b =.33, r = 10,
k = .0173

1. *Behaviour of the normal pathway*

Two negative feed back pathway

r =10 α_1=1 α_2=0.01 α_3 =0.01
g=4 and n=2.

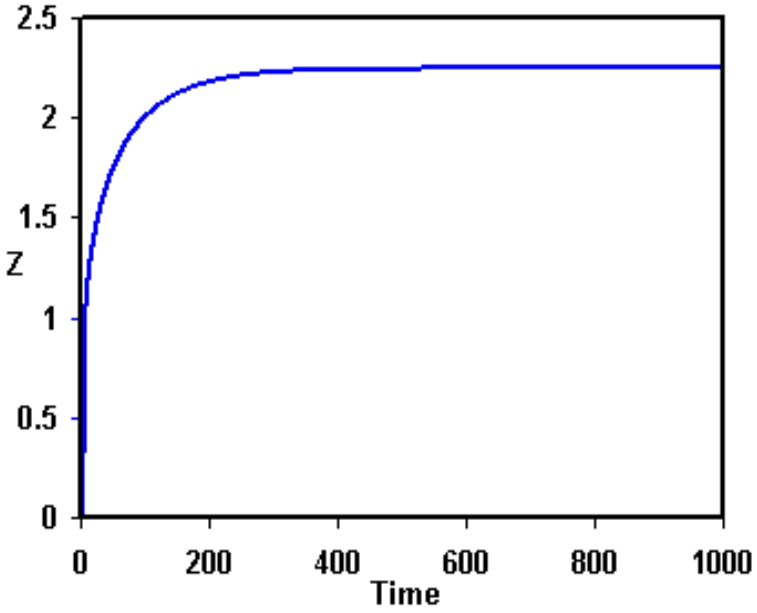

Single negative feedback pathway

(β = 0.33 and k= 0.0173)

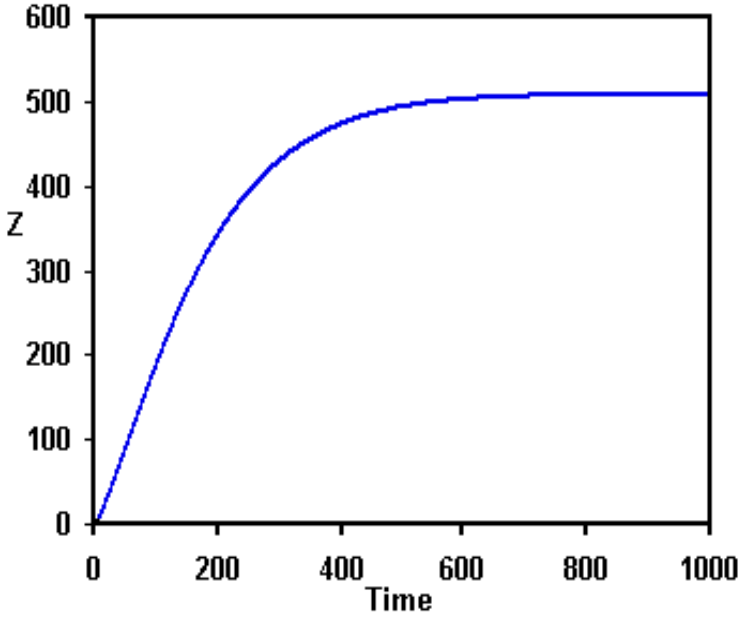

Both pathways are stable under normal values of parameters. But he amount of end product produced is much less in dual negative feedback design.

2. *Changing strength of repression, γ:*

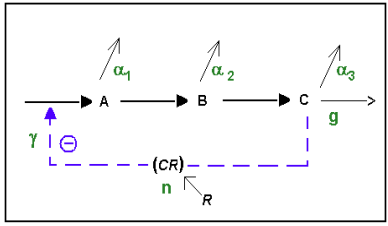

Stable steady state, r =100

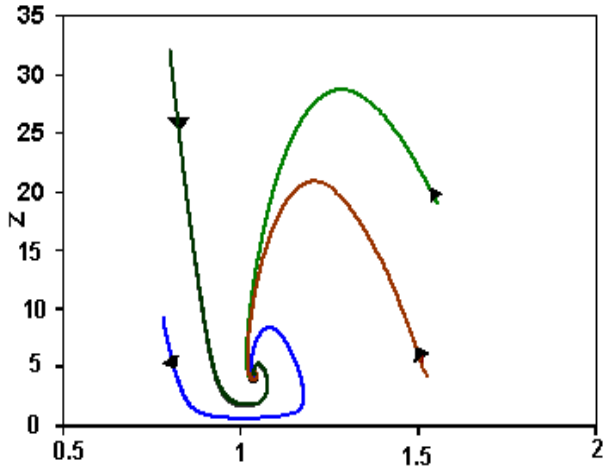

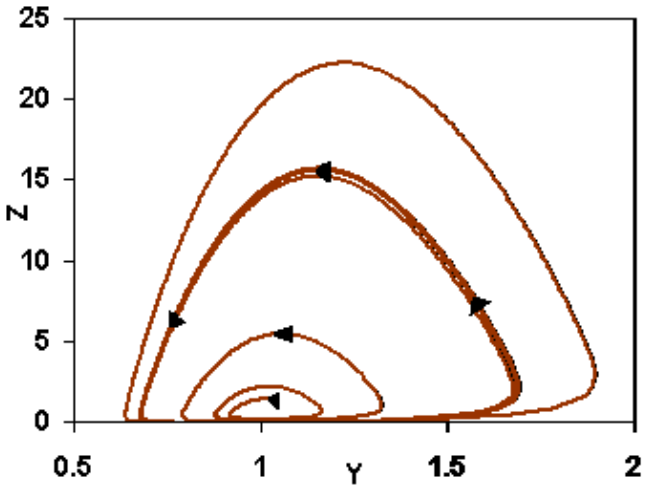

Stable Limit Cycle, r = 500

Bistability, r =250

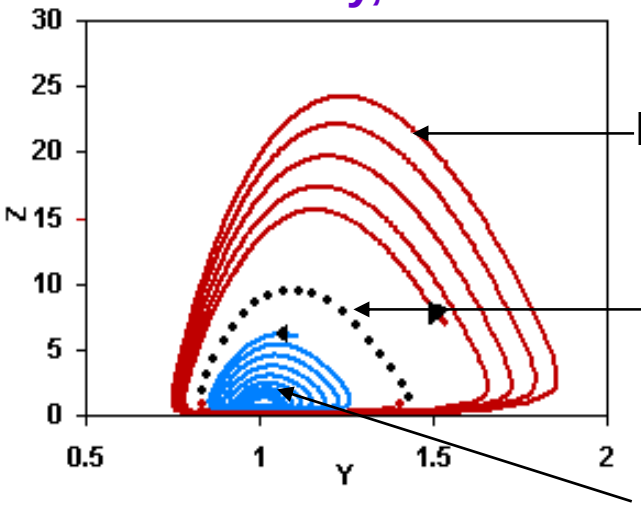

Limit cycle

Seperatrix

Equilibrium point

On increasing repression, the pathway loses stability via a sub-critical Hopf bifurcation, and exhibits bistable behaviour for a range of parameter values.

No change in dynamics on 100-fold increase in γ in dual negative feedback design

3. *Effect of random perturbation on dynamics*

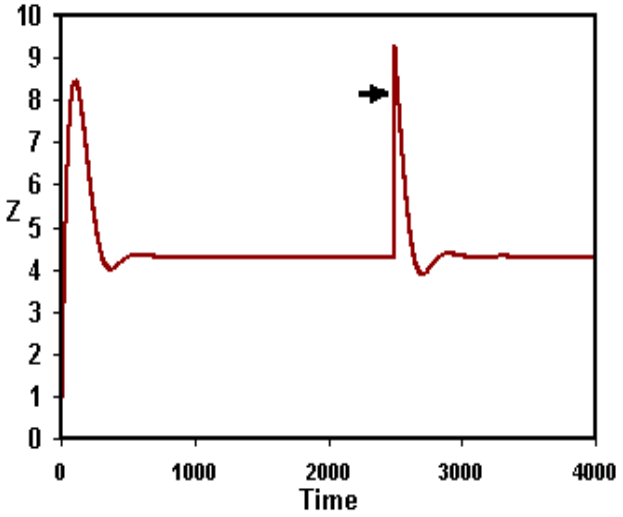

In stable region: γ=100. *No effect.*

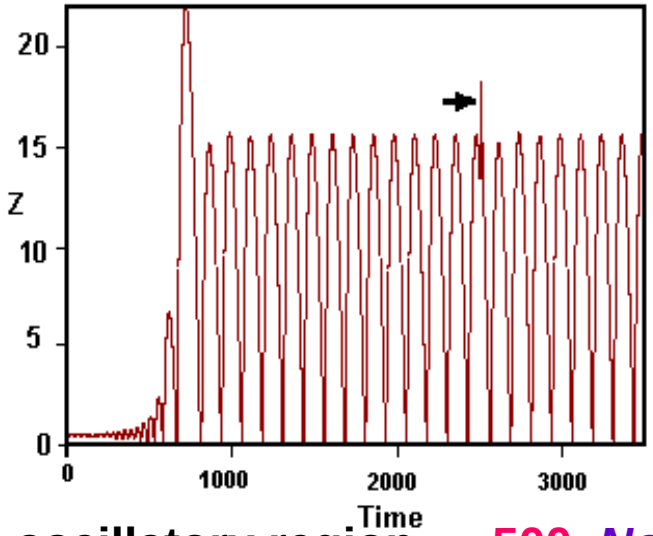

In oscillatory region: γ=500. *No effect.*

Bistable region: γ =250

Small perturbation.

No effect

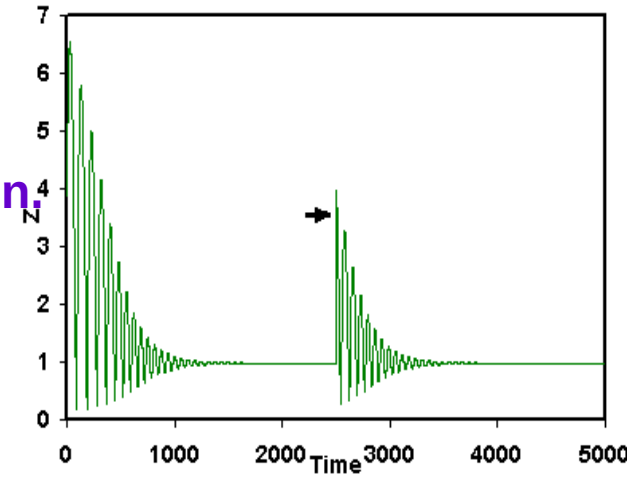

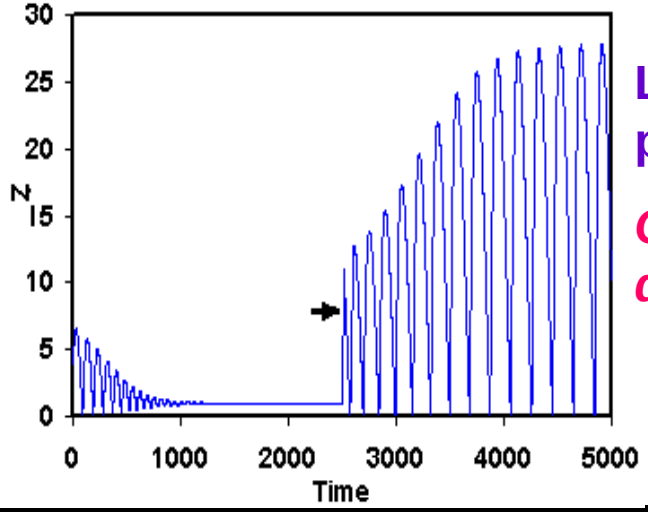

Large perturbation.

Change in dynamics

Pathway dynamics depends on strength of perturbation

3. Effect of instantaneous perturbation

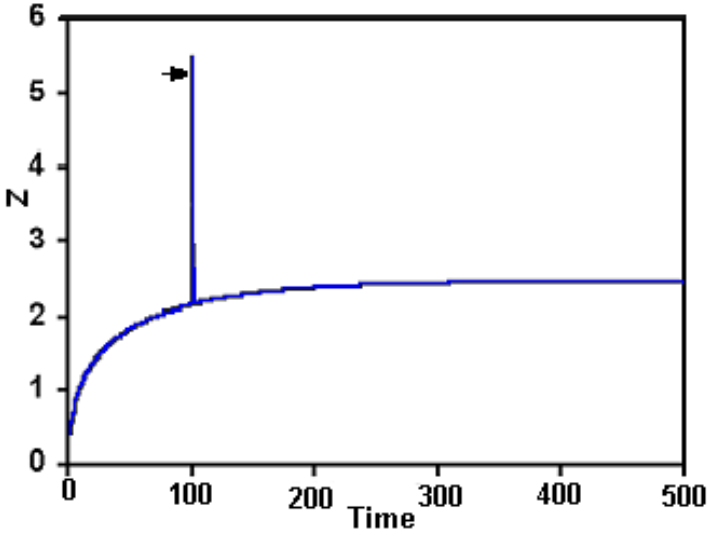

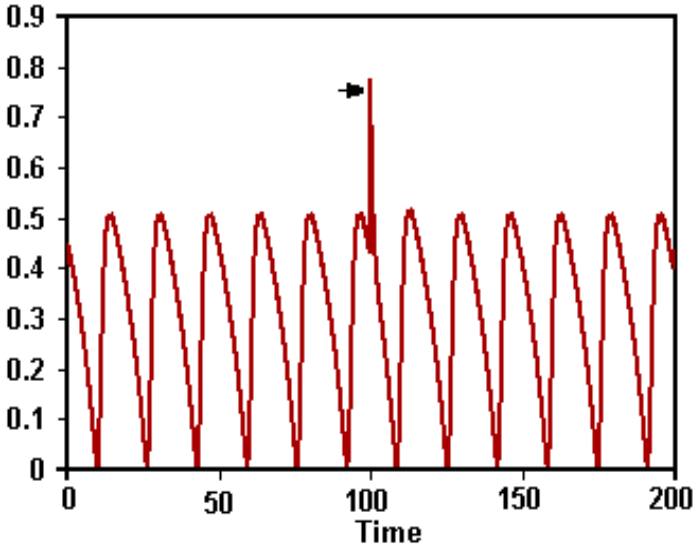

In stable region: γ = 10.

No effect of perturbation.

In oscillatory region: γ = 3500, k = 0.

***No effect of perturbation*.**

The pathway is robust to random perturbations in end product concentrations (experimental noise).

Prediction for over-production of Tryptophan

in reduced inhibition background

g ↓ Z ↑

almost doubles production

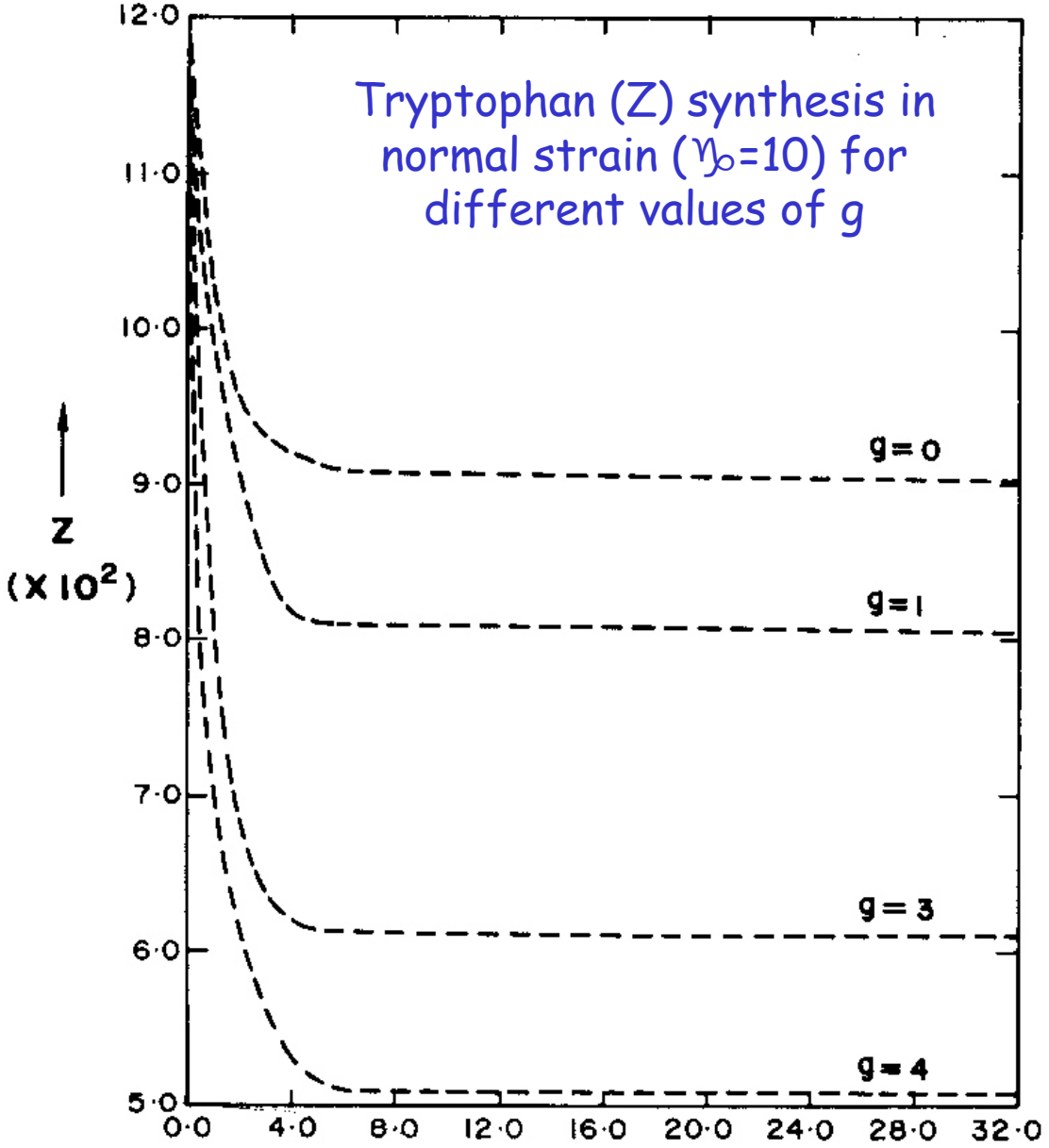

Predicted mutations –

- ***Reduced Asase binding to Trp***
- ***Reduced incorporation of Trp in protein synthesis***

Prediction for over-production of Tryptophan

Tryptophan (Z) synthesis in normal strain for different values of g

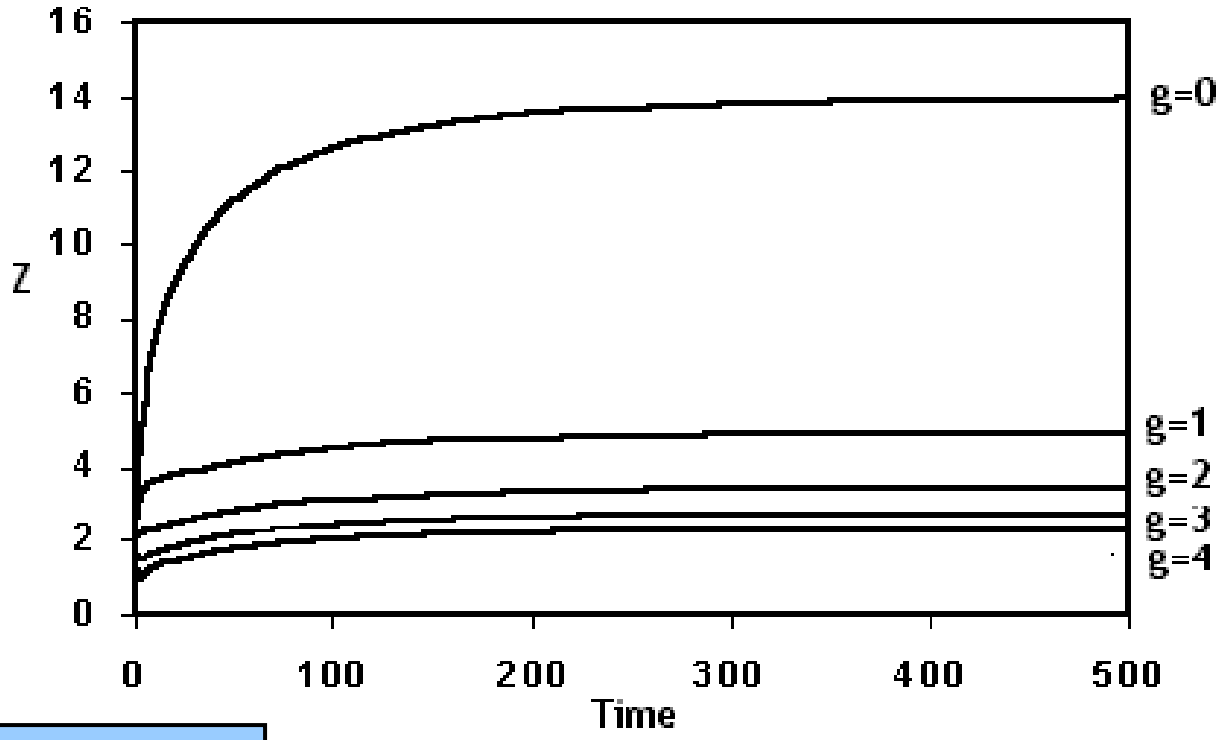

In wild-type background

g ↓ Z ↑

Increase in synthesis is ~ 7 times

Predicted mutation –

- ***Reduced incorporation of Trp in protein synthesis***

Expression of the tryptophan operon of E.coli :

Strain W1485 trp^-

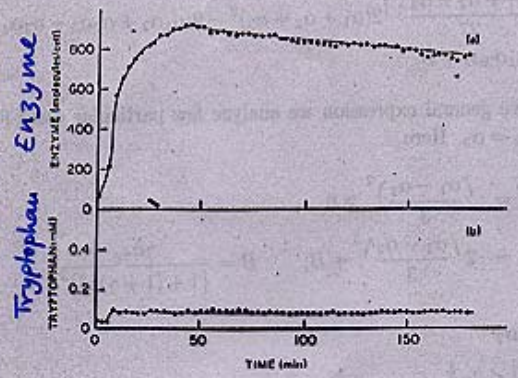

normal feedback inhibition on Asase

Strain 1-42

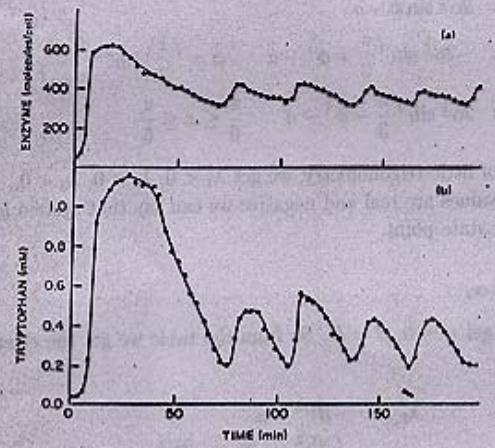

reduced feedback inhibition

Bliss, et.al. 1982 J. Theor. Biol.

For wild type parameters

n = 2, a1 = 1.0,
a2 = a3 = 0.01,
g= 4, γ = 10

The steady state values are

A=0.5,
B=866.5
C=0.03.

A MODEL BIOCHEMICAL PATHWAY

having positive and negative feedback processes

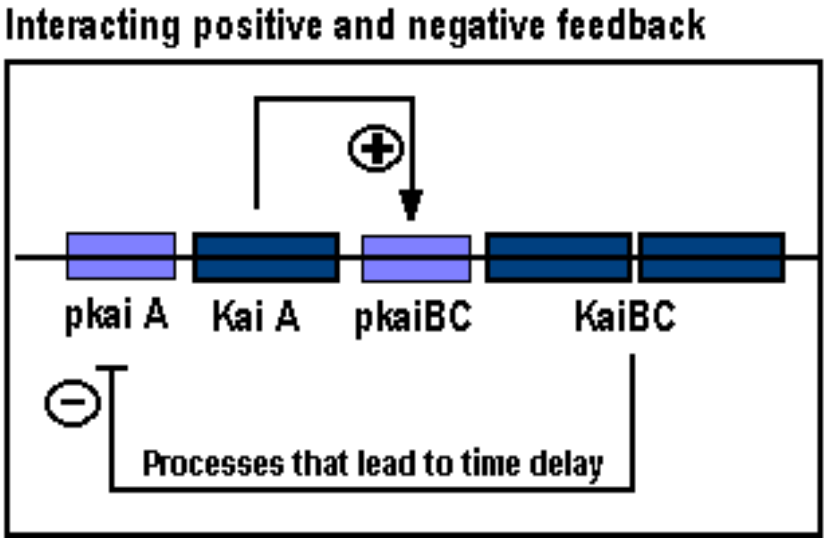

Process for circadian rhythm generation in the yanobacterium, (Synecococcus). Ishiura et al, Science(1998), 281,1519

End-product inhibition coupled to allosteric auto-activation

(positive and negative feedback)

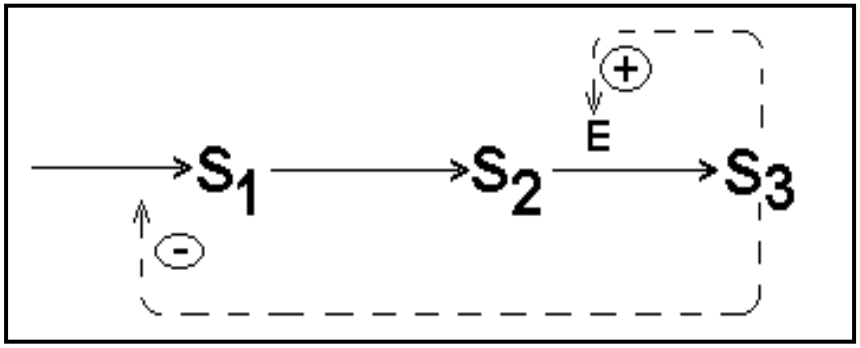

$$\frac{dx}{dt} \equiv f_1 = F(z) - kx$$

$$\frac{dy}{dt} \equiv f_2 = x - G(y,z)$$

$$\frac{dz}{dt} \equiv f_3 = G(y,z) - qz$$

with

x, y, z - normalised concentrations of S_1, S_2 and S_3

k and q - rates of degradation of S_1 and S_3,

F(z) inhibition function for S_1 by S_3. → $F(z) = \frac{1}{(1+z^n)}$

(Co-operative binding of n molecules of z)

Positive feedback term G(y,z) involves the *allosteric enzyme E* → $G(y,z) = \frac{Ty(1+y)(1+z)^2}{L+(1+y)^2(1+z)^2}$

The parameter values are from similar naturally occurring pathways.
Normal parameter values are: n=4, L= 10^6, T=10, k=1, q=0.01

The normal (wild-type) **pathway exhibits equilibrium dynamics**

Negative feedback

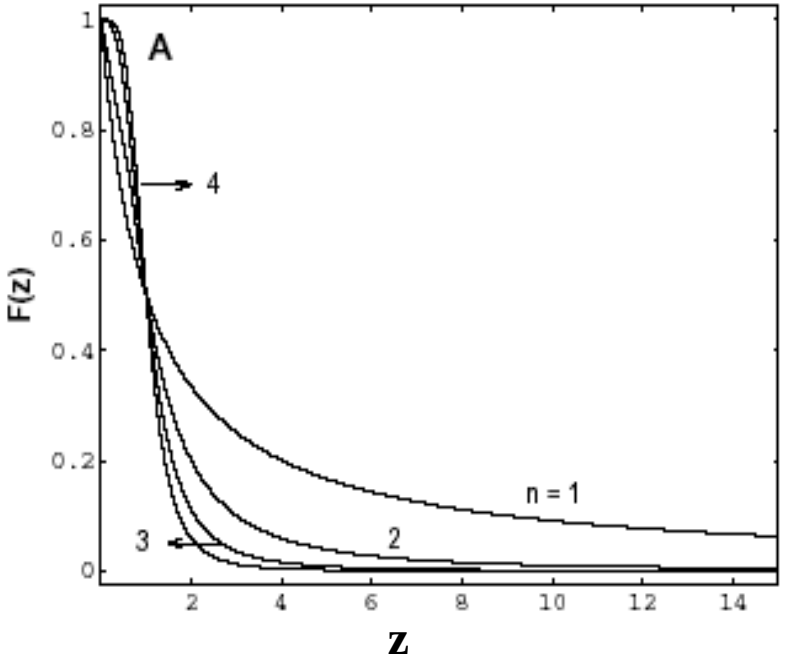

Repression is switch-like for higher n

Positive feedback

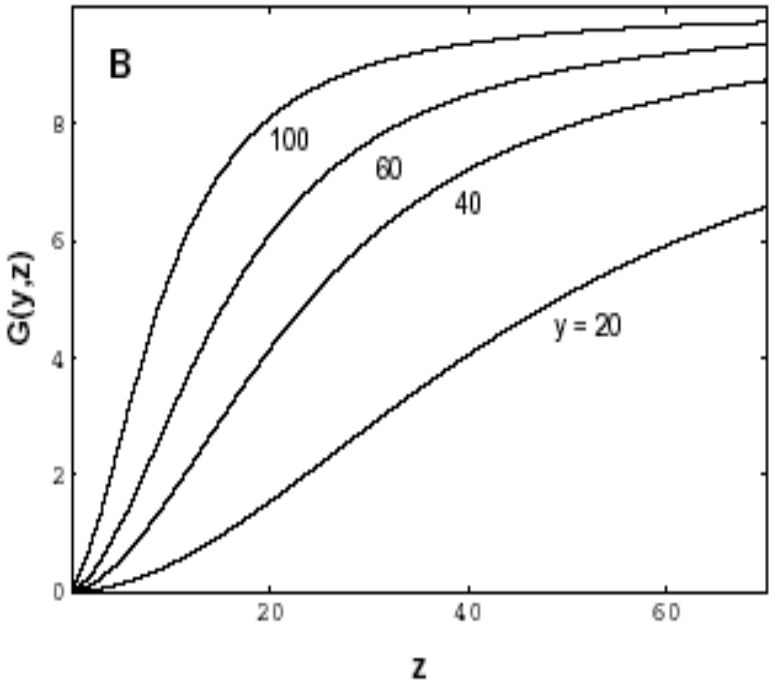

Activation reaches saturation faster for lower z at higher conc. of y

1. Effect of change in two parameters.

Effect of co-operativity (n) on the stability in k-q (degradation rates) space

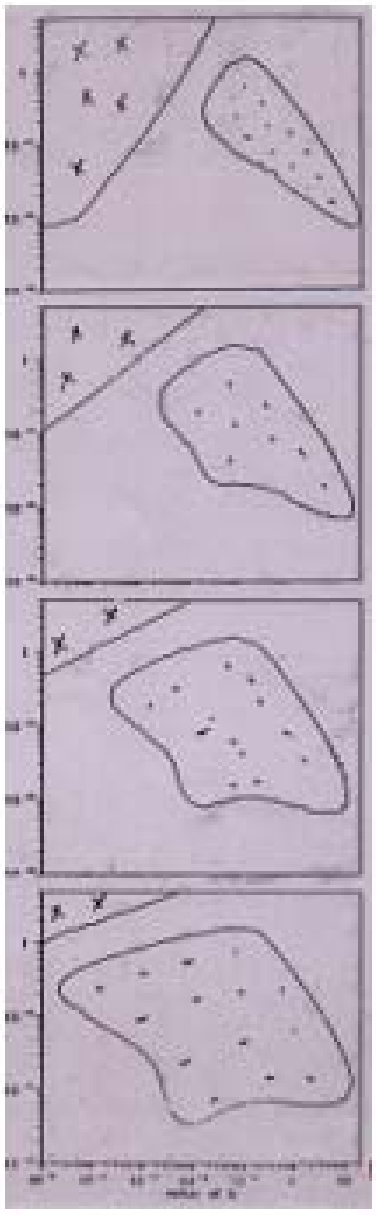

Bifurcation analysis shows that

As the cooperativity in the negative feedback reaction increases,

the pathway shows unstable dynamics in larger range in the k-q parameter space.

□ → Stable

⁘ → Inadmissible

× → Unstable

The stability plots for the pathway on changing both rates of degradation k & q

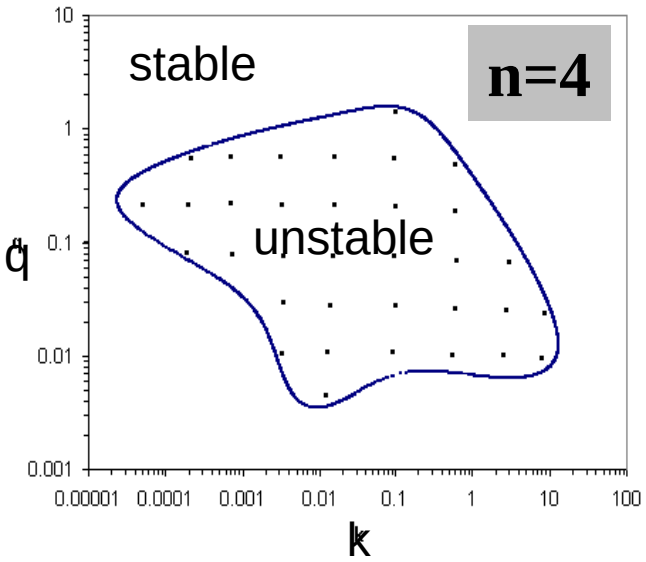

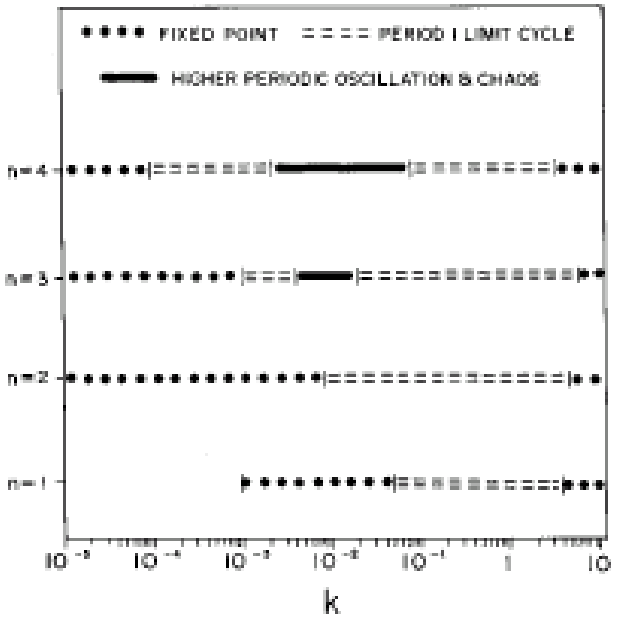

In the unstable region, the pathway shows a variety of dynamics for different k and q.

Bifurcation diagram with 'k'

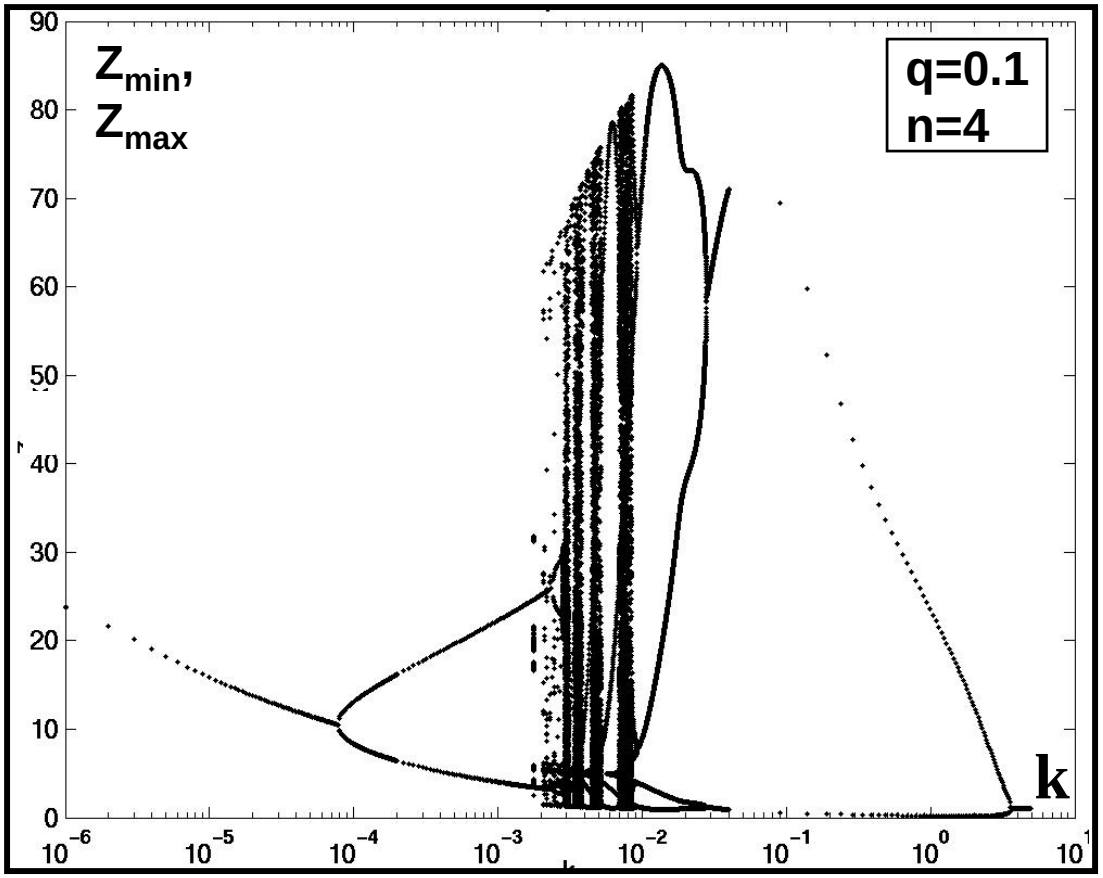

The pathway shows -

Equilibrium and *periodic dynamics* for low and high k, *period doubling, birhythmicity* (co-existence of two different limit cycles), *limit cycles of higher periods, complex oscillations & chaos* for a small range of medium values of k.

2. Characterisation of the chaotic dynamics in the pathway

Chaotic attractor

time series and phase plot

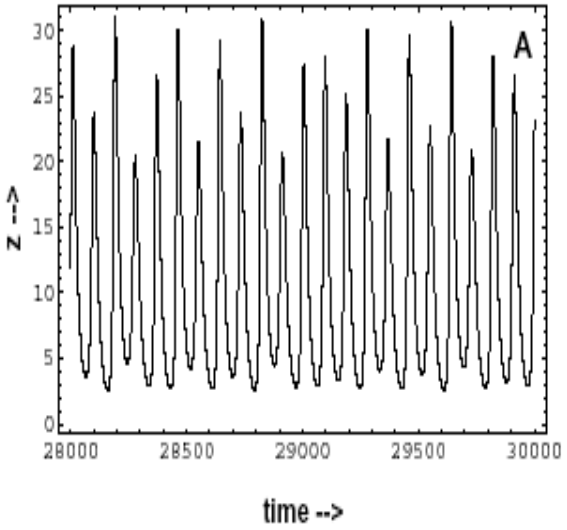

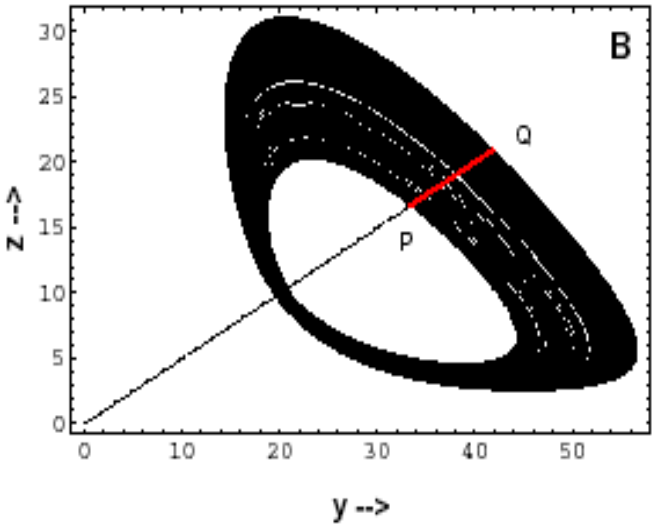

Poincare section

Single hump

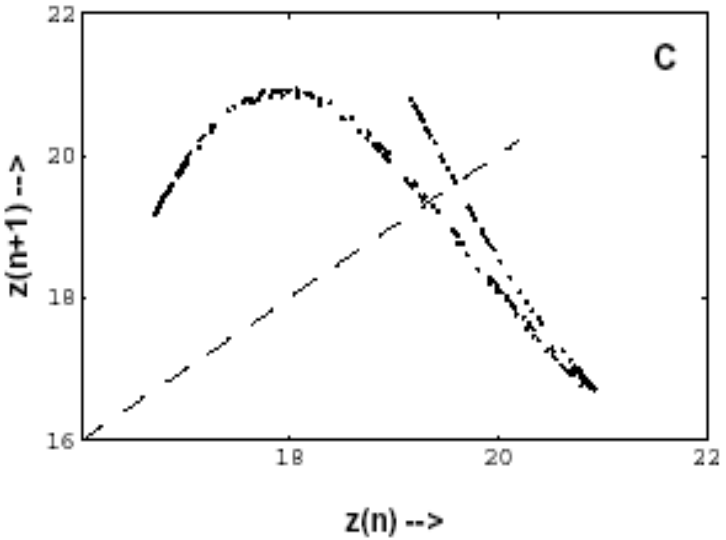

2. Characterisation of the chaotic dynamics in the pathway (contd.)

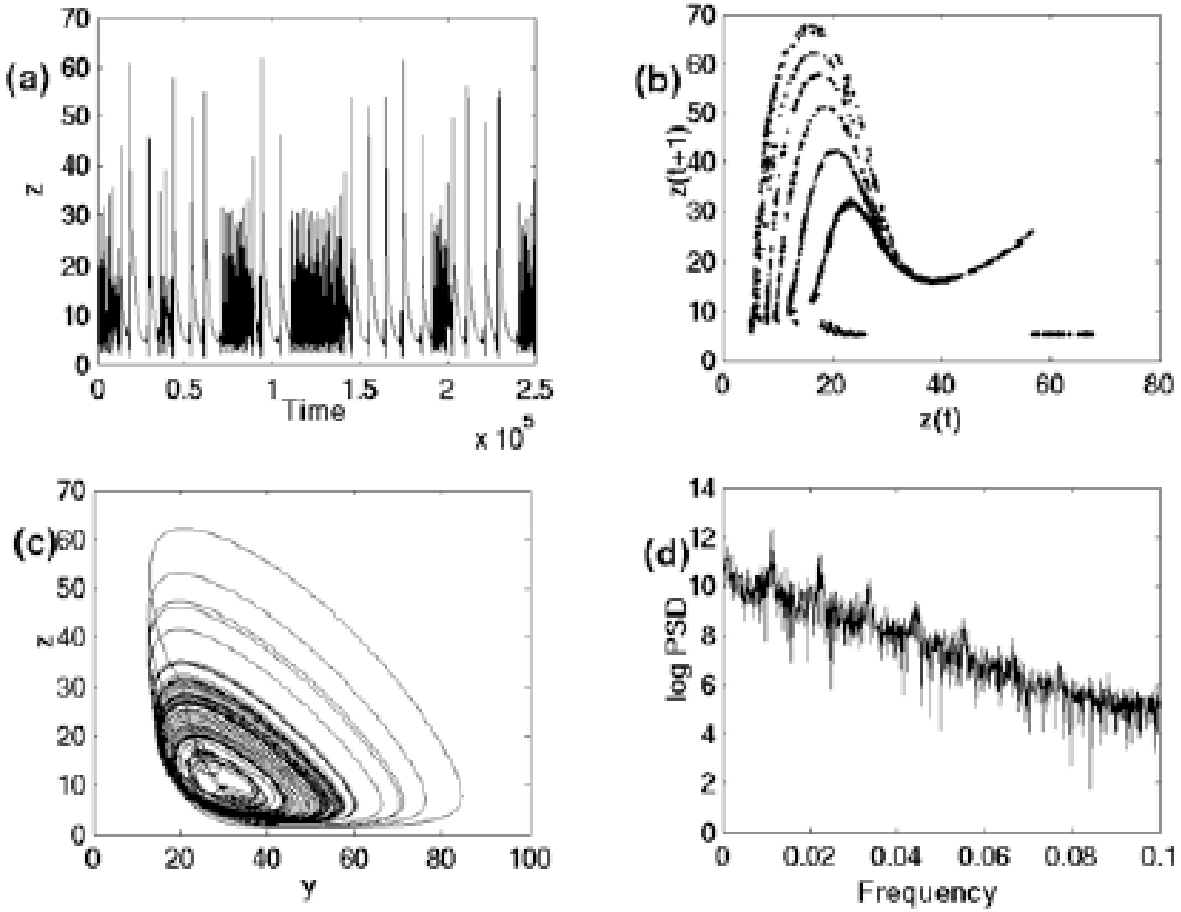

3. Behaviour of the pathway in the birhythmic regime (k=.0024, q=.1)

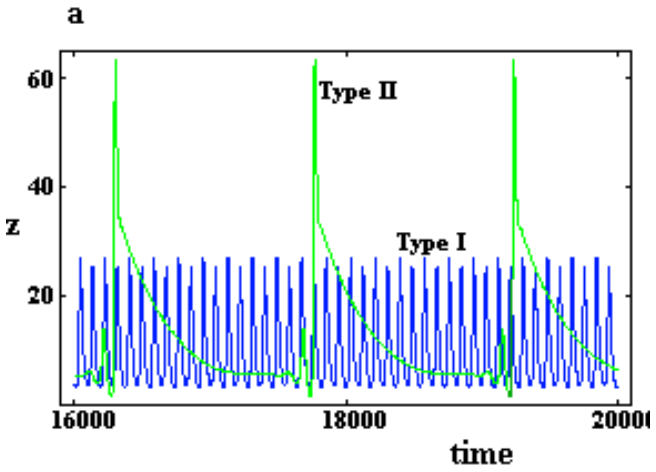

Time series

The co-existing limit cycle attractors

Type I

period doubled limit cycle with small amplitude and time period

Type II

with large amplitude and time period

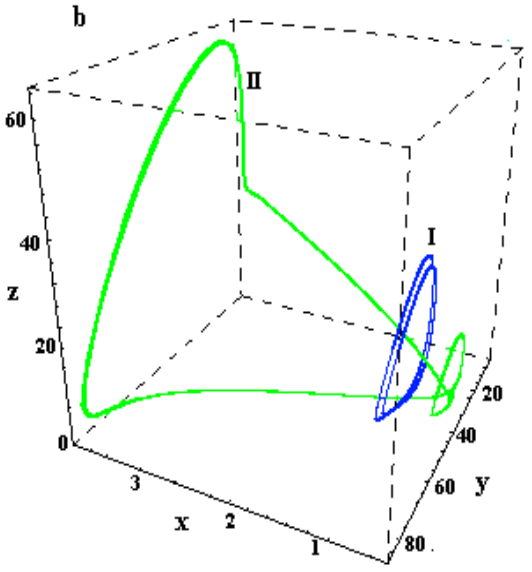

3-dimensional phase plots

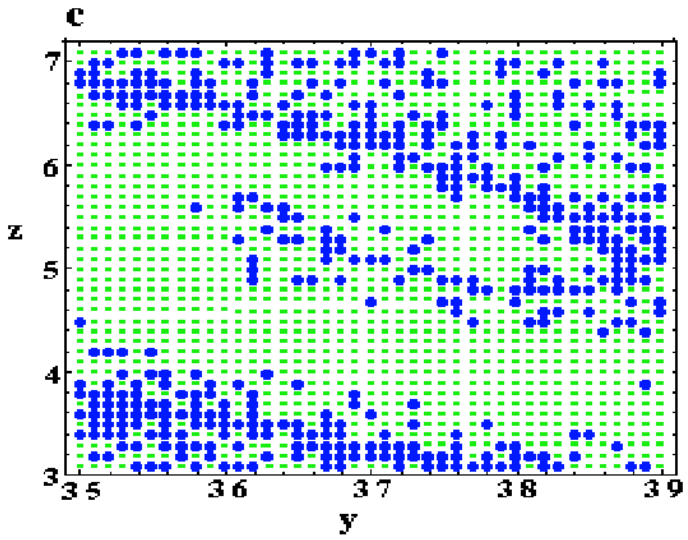

The basin of attraction of the two attractors around the fixed point is fractal

Effect of noise on the pathway dynamics in such situations ?

4. Effect of noise on the pathway dynamics

Effect of single perturbation of variable strength to the end product, z, at t = 6000.

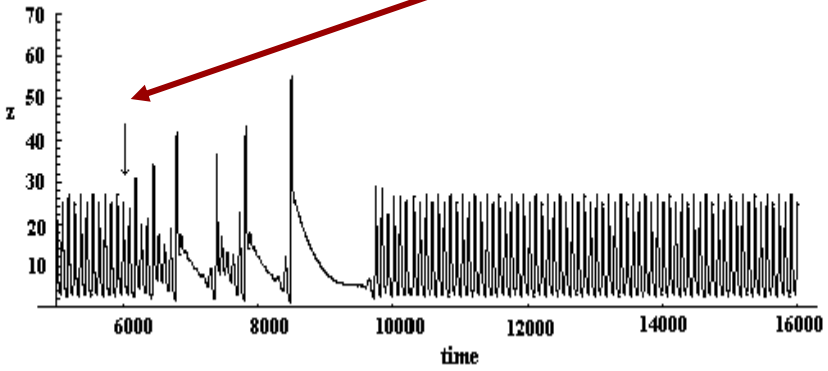

Resultant dynamics continue to be of the same type

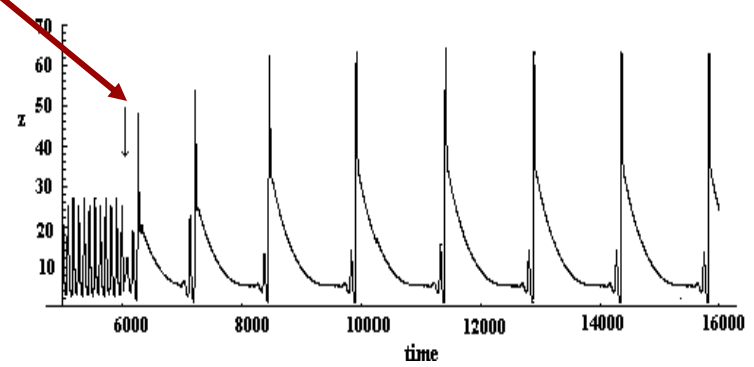

Resultant dynamics change to the other type of attractor

Resultant dynamics exhibit super transients

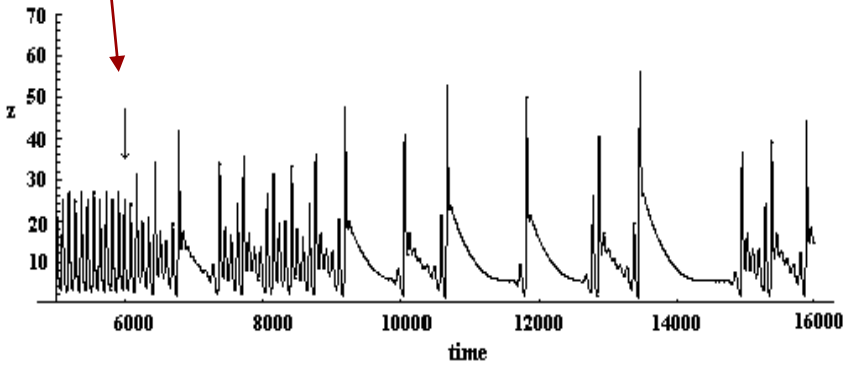

Unpredictability in dynamics under noise

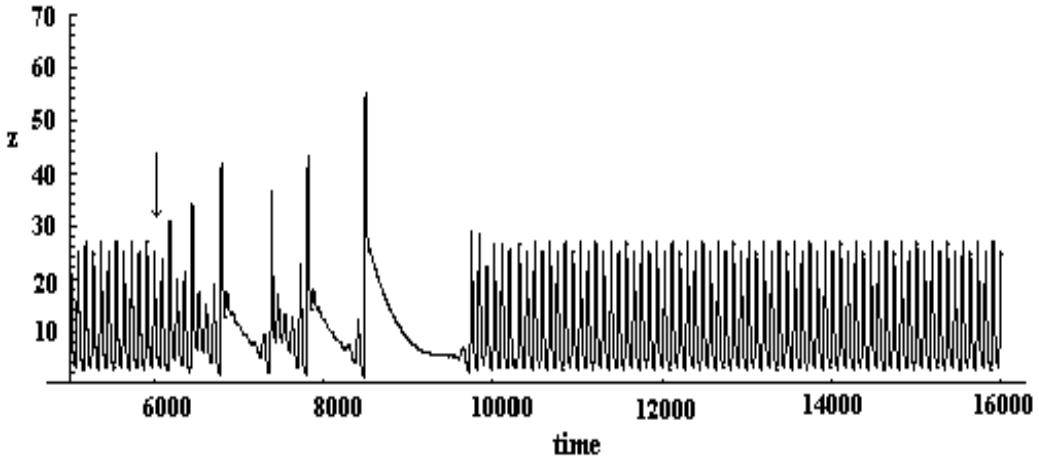
70
60
50
40
30
20
10
z
6000
8000
10000
12000
14000
16000
time

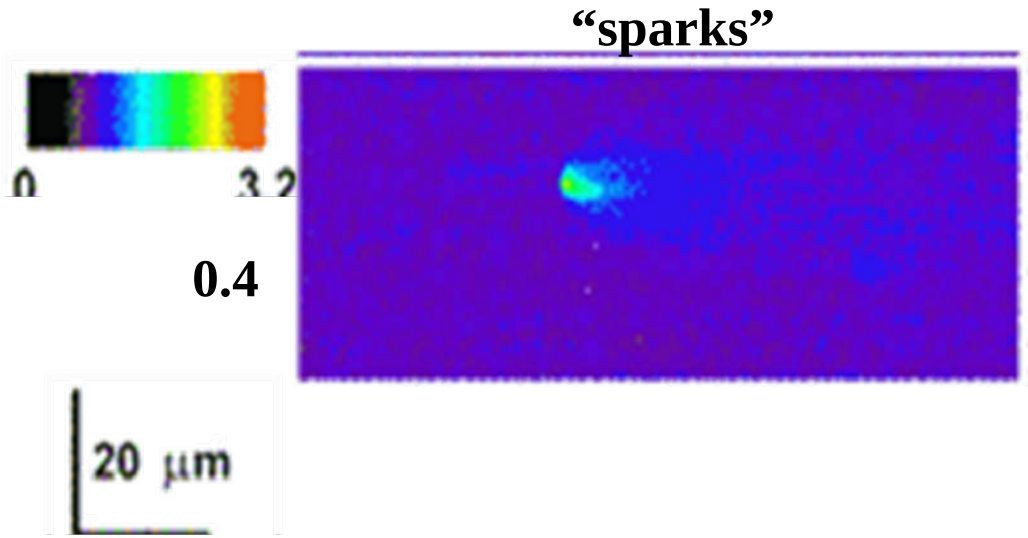
“sparks”
0
3.2
0.4
20 µm

5. Phase Sensitivity of the Pathway Dynamics to Single Perturbations

- There is considerable overlap of the attractors in the phase space
- Final evolution of pathway does not depend on strength of perturbation
- The basin of attraction is fractal

How is the pathway dynamics dependent on the phase & strength of perturbation ?

Type II attractor

3D phase plot

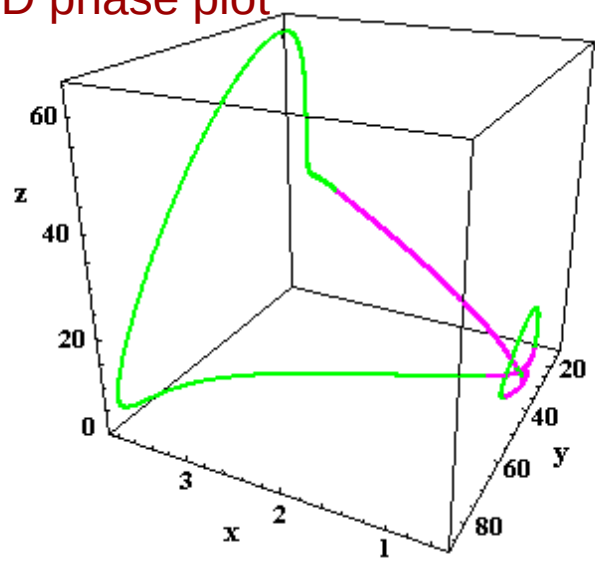

Time series

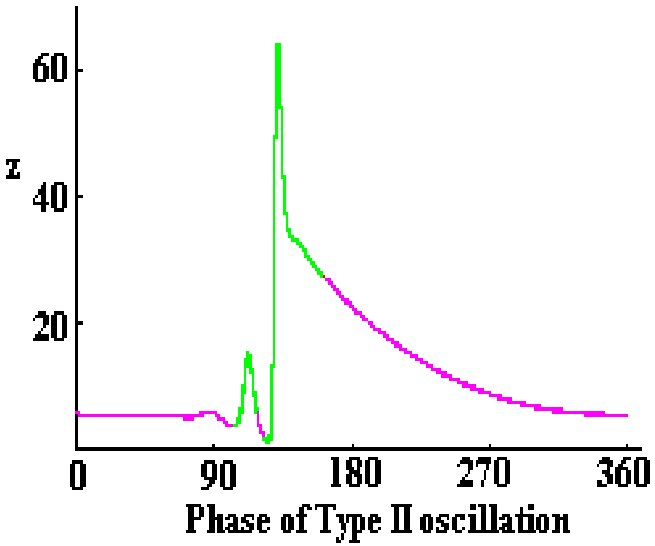

Type I attractor

no clear separation of sensitive and robust phases

Phases sensitive to perturbation

6. Effect of parametric noise in the birhythmic region, k= .0024, q = .1

(Controls - in the absence of noise)

Type I limit cycle

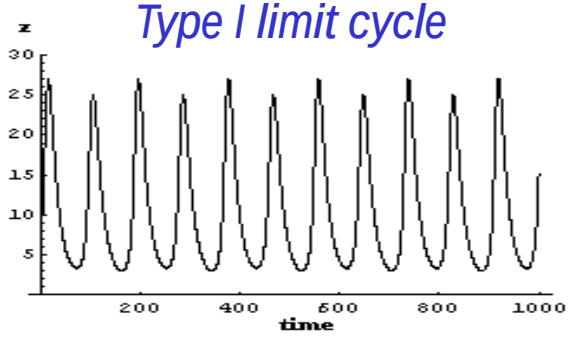

Power spectra

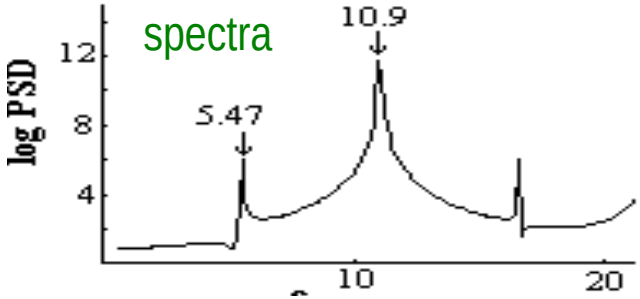

Type II limit cycle

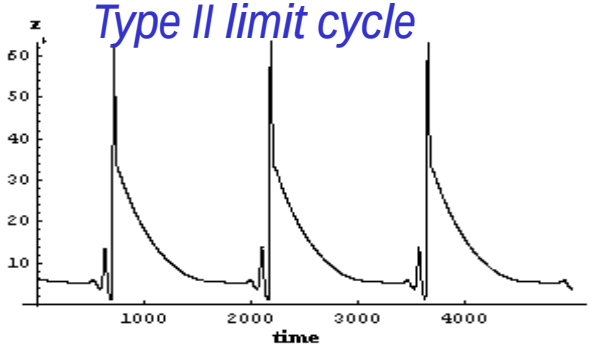

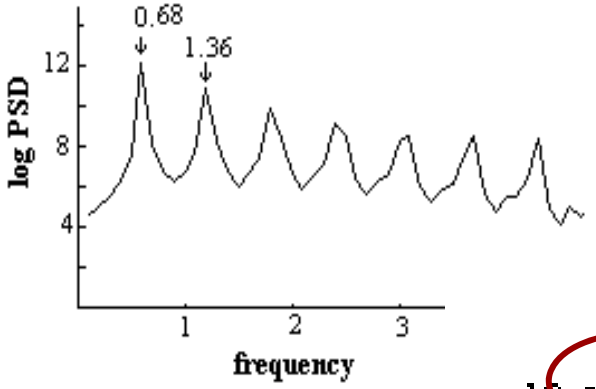

The co-existing limit cycles have very different frequencies & amplitudes

Power Spectra under noisy k

(q=0.1 + σ)

σ- Uniform[-0.005, 0.005]

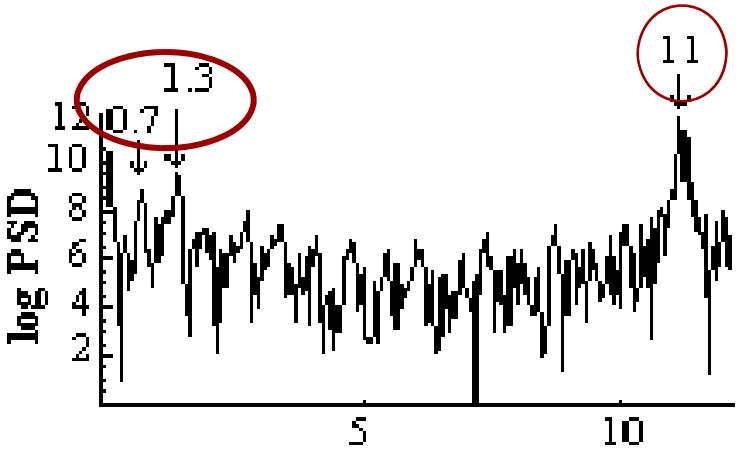

Even small amount of noise can mask the intrinsic dynamics

Effect of parametric noise in the regions showing simple periodic states

$(q = 0.1 + \sigma)$

$\sigma = 0$

σ – Uniform[0.05]

Power Spectra of the limit cycle attractors

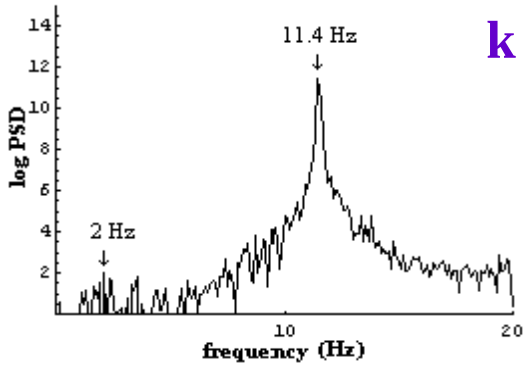

k = 0.001

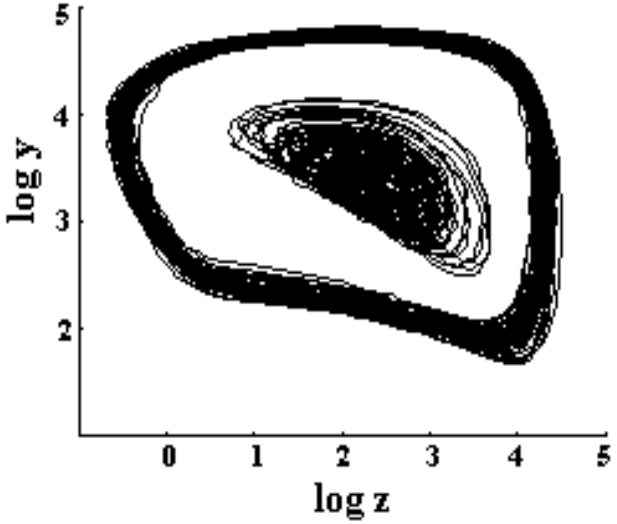

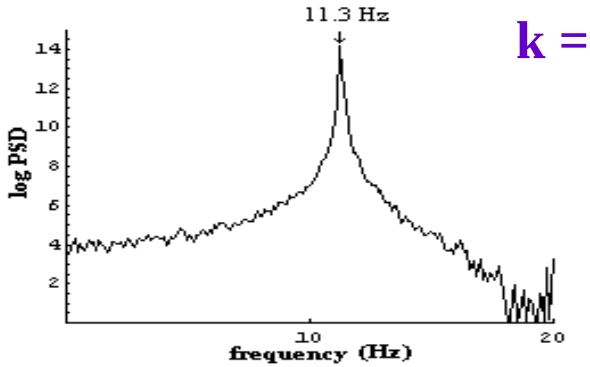

k =0. 07

Intrinsic pathway dynamics is observed even under large amount of noise.

Conclusions

1. **The single negative feedback pathway is more flexible in the range of dynamics that it exhibits than the pathway with two negative regulatory processes.**

2. ***Comparison of the two arrangements of negative feedback clearly shows the advantages conferred by the additional feedback in terms of increased stability to mutation and environmental noise.***

3. **The source of this stability is likely to be in the second feedback, since it is effective immediately.**

4. ***Addition of a positive feedback to the single negative feedback pathway induces instability and exhibits a wide variety of dynamical behaviour for parametric changes.***

5. **Environmental and systemic stochasticity can expose and/or conceal the dynamical properties of the pathway.**

6. **The existence of birhythmicity in this pathway with fractal basin of attraction for some ranges of parameters can lead to –**

   (a) Unpredictable final state –

   The efforts to produce clonal or identical output will "always find an irreducible level of random variablity" ***Mcadams & Arkin, 1997***

   (b) Perturbation induced switching mechanisms that select between alternative regulatory paths as seen in many clonal or isogenic bacterial populations

   Spudich & Koshland, 1976; Schwann, et al, 1992

7. ***This pathway exhibits both noise-sensitive and robust behaviour under noise in parameters under different conditions.***

8. **Many biological processes (e.g., Calcium oscillations in heart or muscle cells) show spontaneous "sparks" and "puffs" – Transient signalling**

9. **Amplitude and frequency-coded signalling by the same molecule for diverse cellular processes.**

   Using specific combinations of oscillatory controls to trigger different cellular processes ***Meldolesi, 1998; Dolmetsch, 1998***

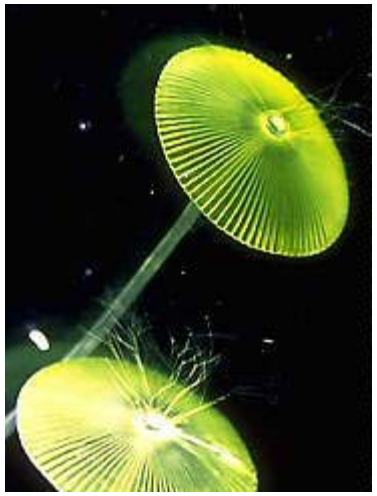

R. Maithreye,

C. Suguna

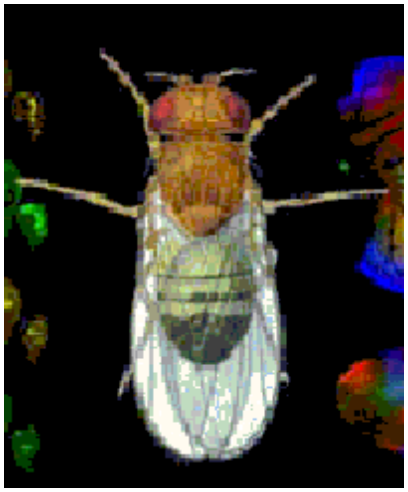

Physica A 2005.

In: ***Function and Regulation of Cellular Systems: Experiments and Models***, Birkhauser, 2003

Fluctuation and Noise Letters, 2002

In: ***Recent Research Developments in Biophysical Chemistry***, 2002.

Physical Review E, 1999.

***Biotech. & Bioengg.,* 1988**

J. Theor. Biol., 1988

Biosystems, 1987

In: ***Chaos in Biological Systems***, Plenum Press, 1987

Modelling Spatially-Extended Biological Systems

Spatially-Extended Biological Systems

Structured group of cells (Tissues/Organs)

Whole organism

Spatially-distributed populations

Cell Assemblies

Social Groups

Spatial Pattern

Spatiotemporal Pattern

Collective Behaviour



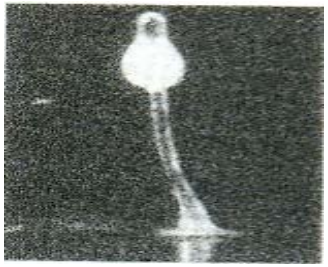

Pattern Formation

Morphogenesis

Development of form starting from near homogeneous initial condition (egg/cell mass)

--> ***involves orchestrated cell division, movement, & differentiation***

Self-organization:

Global pattern emerges solely from interaction among the lower level components of the system.

Cell colonies/Organisms - **slime mold aggregates**

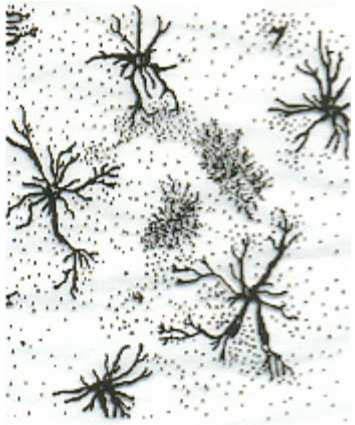

Density-dependent cell population behaviour

Community Effect, Quorum Sensing, Biofilm

Coupled-cell organisation in living systems

Community Effect **Quorum Sensing** **Biofilms**

Population of similar cells emit a signal factor.
Only when the number of cells reach a certain density,
they respond to this factor and induce new gene expression.

Community Effect : **Developmental signalling in embryos -**
Induction of differentiation in cells by neighbouring cells

Quorum Sensing : **Auto-induction of luminescence in light-emitting marine bacteria at high density only.**

Biofilms: **Groups of pathogenic organisms secrete toxin only above certain cell density in the layer - presumably to avoid killing by immune system and attack with increased toxic load.**

TWO MOST IMPORTANT FEATURES OF

A COUPLED SYSTEM

COUPLING

(INFORMATION TRANSFER & TYPES OF INTERACTIONS)

&

GEOMETRY

(LENGTH, BOUNDARY & BOUNDARY CONDITIONS)

Modes of Communication Between Cells

(Coupling)

Other Types of Communication

Active or aided by wind/water

Humoral - long distance signalling

sound, light, pheromone, pressure, temperature, migration, dispersal

Receptor-ligand - contact signalling by membrane molecules

Different types of Interactions

Junctions in membranes contact signalling through Gap junction, Tight junction

all-to-all, nearest neighbour, long distance, random

Matrix-mediated

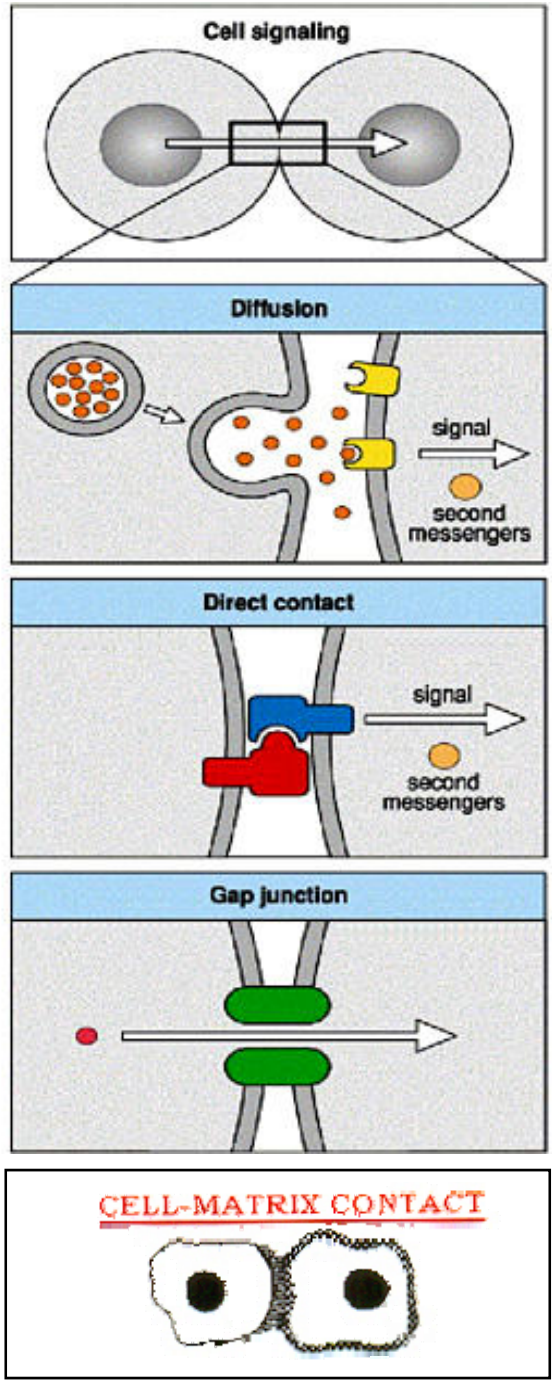

MODELLING THE SPATIALLY EXTENDED SYSTEM

TISSUE OR THE "COLLECTIVE"

Consist of many cells/units interacting in space and time.
The units may be identical or heterogeneous in properties.
The whole system behaviour is "collective behaviour"

Cell Dynamical Systems (CDS) as explicit models for spatially extended systems with many interacting agents in space and time.

COUPLED MAP LATTICE SYSTEMS (CML)

Consider a lattice : **Each lattice node/site represents the Agent with a dynamical system. The Agents interact among themselves.**

Why use this approach ?

Cells in a tissue **are discrete entities having localised dynamics, and are coupled to each other through sharing of chemicals/voltage.**

CASE STUDY

MODELLING ELETRICAL ACTIVITY of BETA CELLS in PANCREATIC ISLETS

Pancreas (5 cm in length in a 20 yr old)

In the abdominal cavity just below the *liver* and under the stomach. It has spleen in one side and duodenum (first segment of small intestine) on the other.

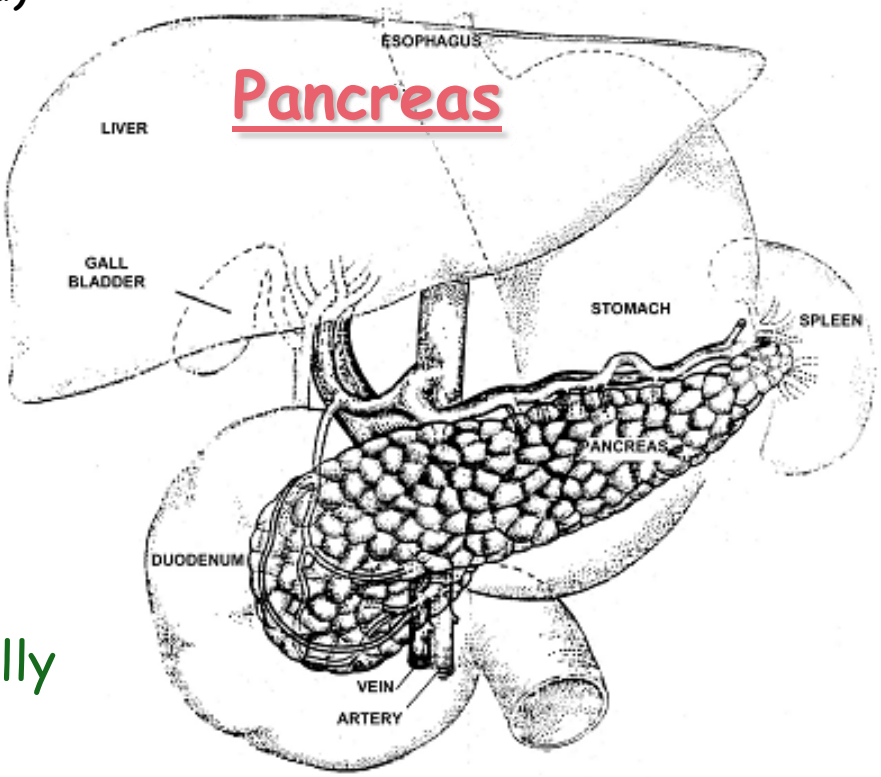

Pancreas is made up of two functionally distinct components:
Acinar cells and **Islets of Langerhans**

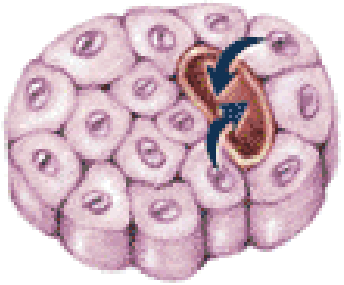

Islets of Langerhans cells secrete hormones into blood vessels

Islets

Diameter: 0.2-0.5mm

Each contains a few thousand cells

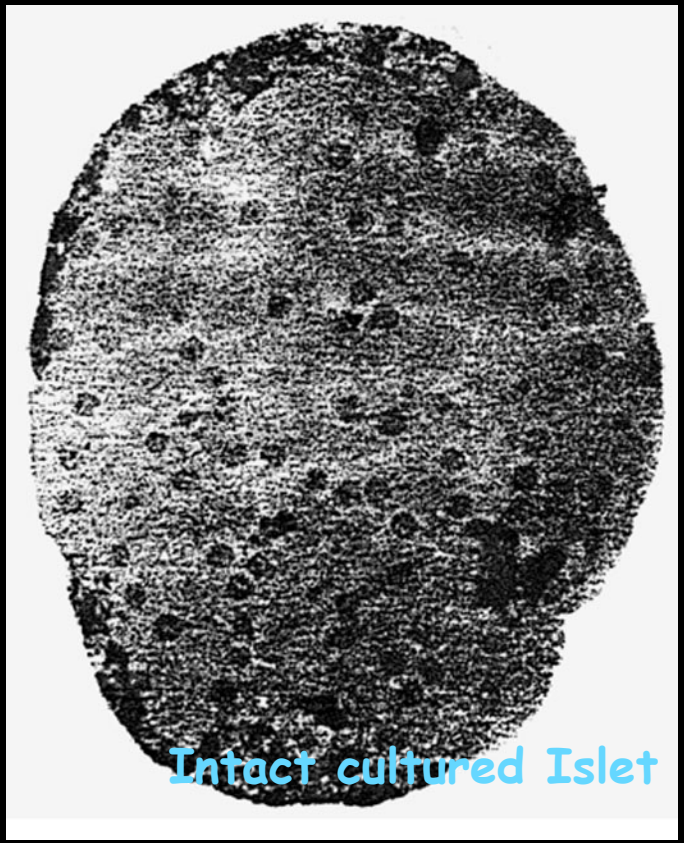

Non random distribution of cells

Beta cells form the core

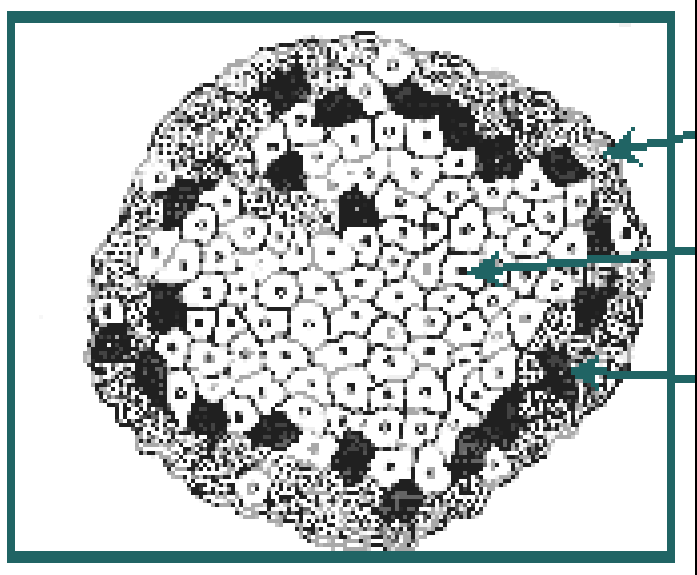

15-20% - ALPHA CELLS - Glucagon

65-80% - BETA CELLS - Insulin

3 - 10% - DELTA CELLS - Somatostatin

1% PP CELLS

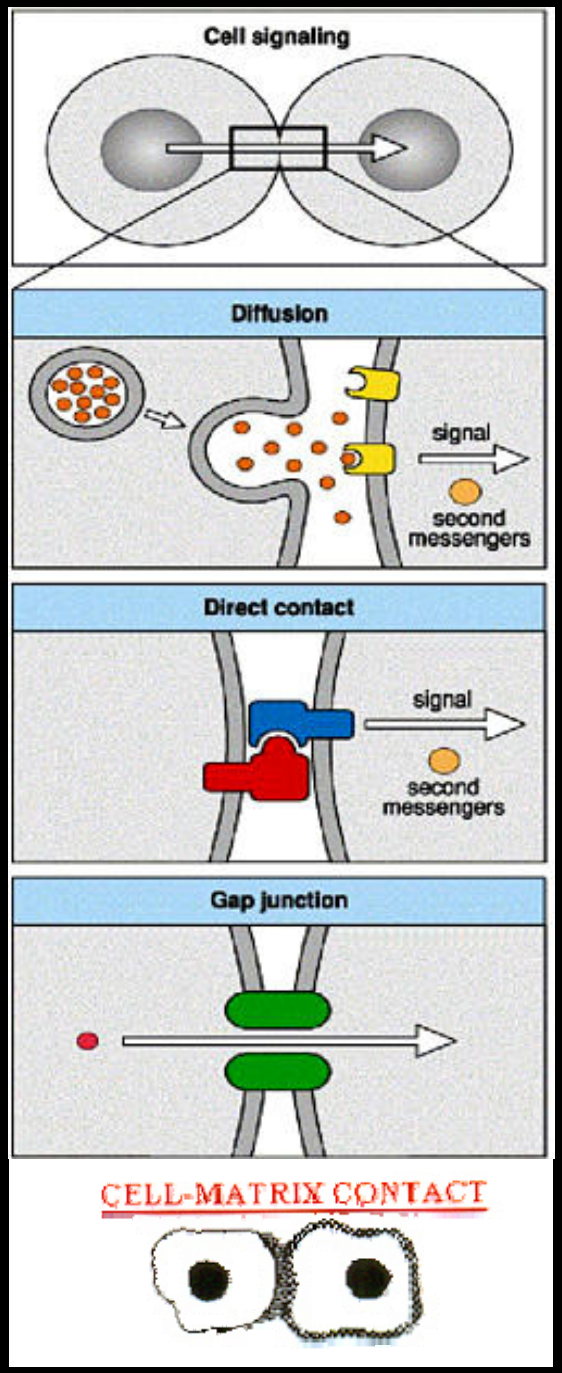

Mode of Communication in Beta cells

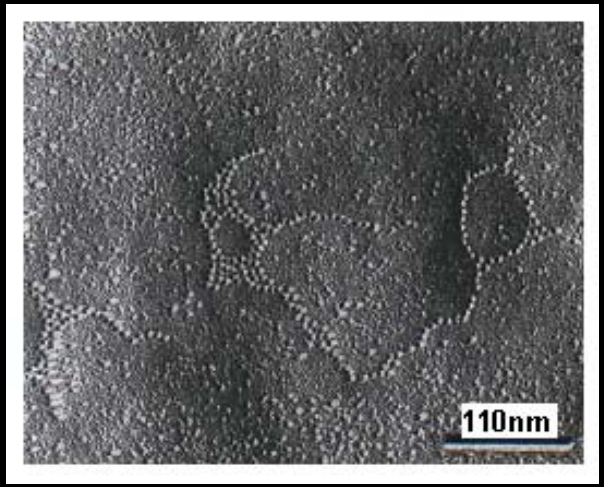

Voltage sharing through Gap junction

Major gap junction protein is Connexin-36

(Meda *et al*, Diabetes, 2000; J. Clin. Invest. 2000)

Bimodal distribution of coupling conductance

26 in-situ cell pair experiments
(Mears, 1995)

2.49 nS (SD 0.25 nS)
and
3.47 nS (SD 0.25 nS)

Range 4.11 - 2.1

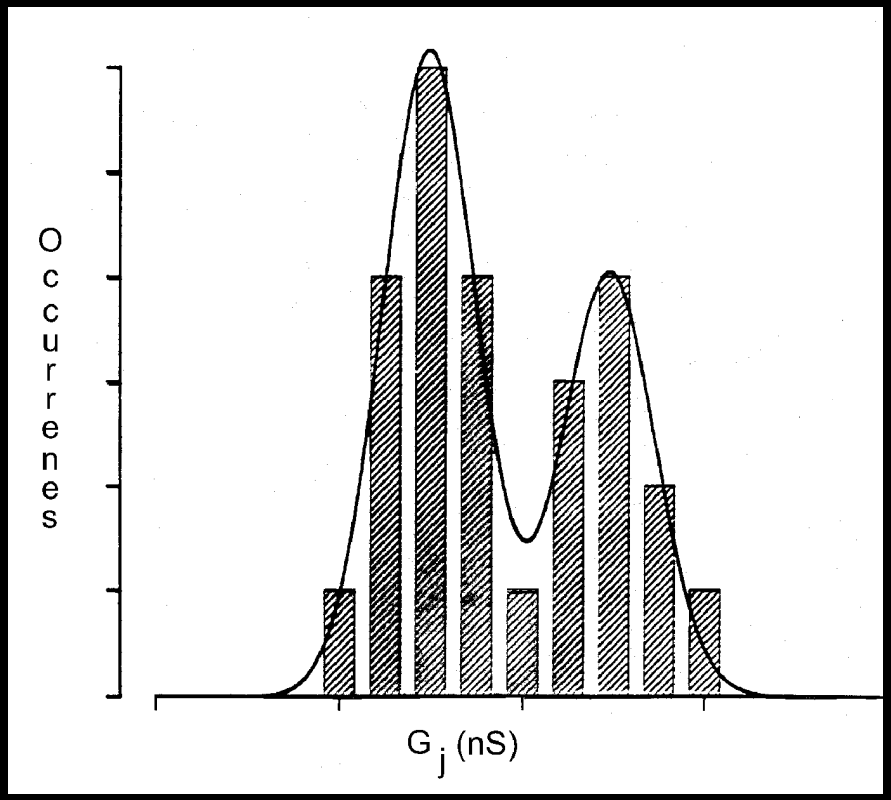

(Meda, 1980)

Non-random distribution of gap junctions in beta cells

β cells at the periphery of islet have twice as many gap junctions than cells at the centre - ~6.97 & 3.47 per 100 sq.μm membrane area

Is there a spatial distribution of conductance ?

FACTS

Several million islets of Langerhans, each contain several thousand cells, secrete insulin in response to the level of glucose in the blood through stimulus-secretion coupling, thereby maintaining the glucose level within a narrow operating range.

Within an islet

β-cells are electrically coupled via gap junctions

Heterogeneity in beta cell properties

Non-random distribution of gap junctions on membranes

Modulation of gap junction distribution by glucose

Release of insulin from beta-cells is **pulsatile** and is correlated with **rhythmic oscillations in membrane potential** –

- Synchronised electrical activity precedes insulin secretion
- Malfunction of electrical activity leads to failure in insulin secretion

Electrical Coupling in Islet Cells

Simultaneous recording using intracellular microelectrode in voltage clamped state at 11.1 mM Glucose

Rhythmic slow plateau waves that depolarise the islets from -45 to -30mV for 10s

Riding on the slow plateaus are rapid Ca^{+2} dependent voltage spikes that further depolarise to -15mV

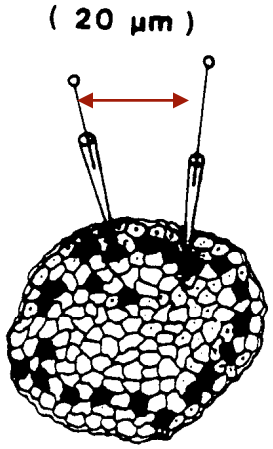

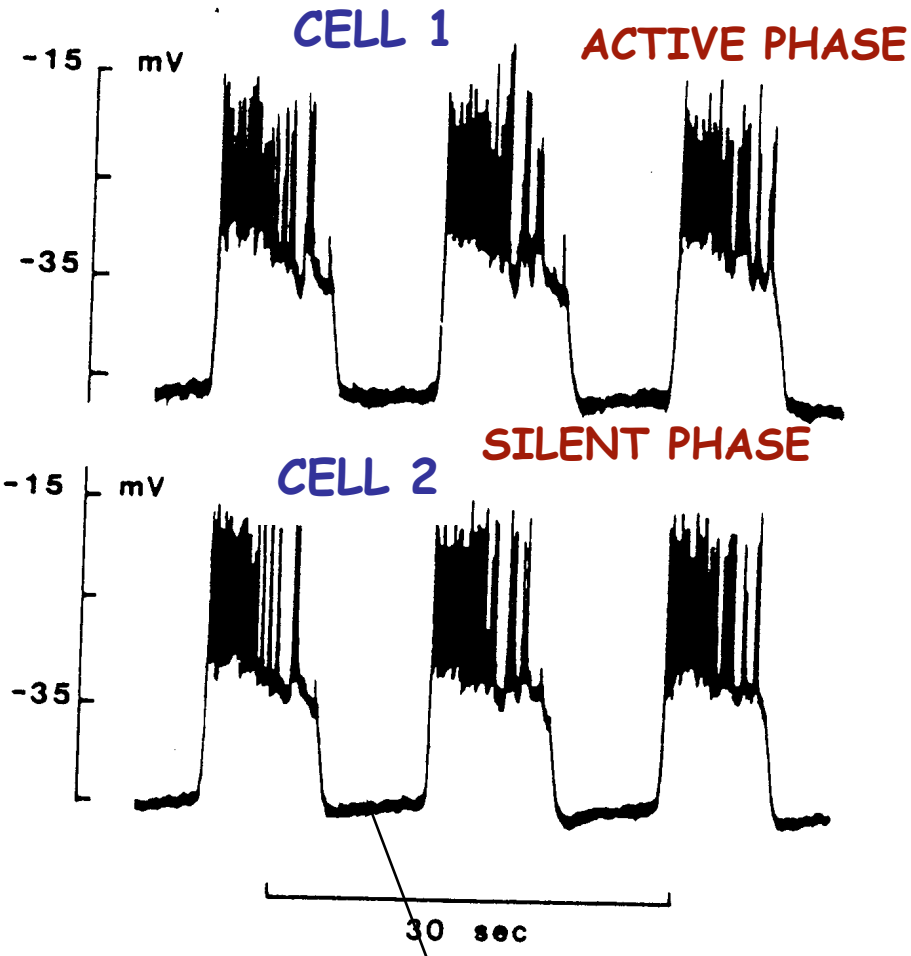

(Eddlestone *et al*, J. Membr. Biol., 1984)

Single Beta Cell Firing Patterns

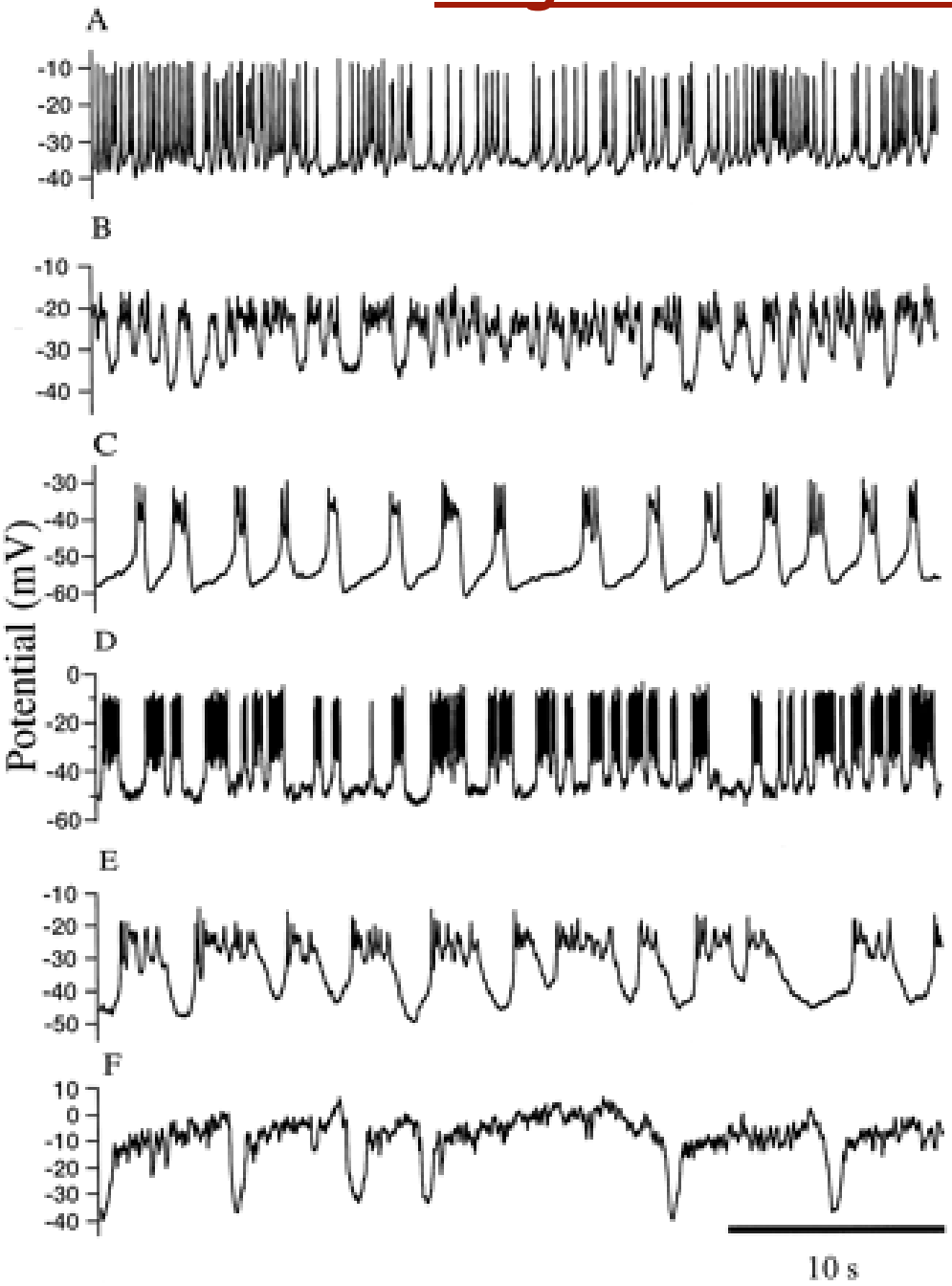

(A) Class I - repetitive fast spikes

(B-E) Class II -
Fast spikes superposed on brief (<5s) periodic depolarizations

These cells show pacemaker potential as is seen in islet bursts

- Silent phases range: -60 to -40 mV
- Plateau phases range: -35 to -10mV

Transition from silent to plateau phase is abrupt in all cases.

One-third are spikers
Half are fast bursters
Period: < 5 sec
The rest are plateau cells

(F) Class III - periodic plateaus of longer (10-20s) duration without clear spikes - Slow bursts with long active phase

(Kinard et al., Biophys J, 1999)

FACTS

- Single beta cells burst over wide time scale
- Coupled beta cells, within an islet, burst synchronously with medium frequency
- Beta cells in the islet have different gap junctional coupling
- The collective interaction of beta cells is critical for their normal functioning in insulin secretion.

How does a collection of beta cells, having a wide variety of bursting frequencies, exhibit emergent synchronised bursts of medium frequency (~25 sec) in the islet?

ROLE OF CELL INTERACTION AND STRUCTURAL ORGANISATION

Model

of the Beta cell

and the Islet

Modelling Electrical Activity in Cells

The plasma membrane maintains an unequal concentration of ions on either side resulting in membrane potential.

Component	Intracellular conc. (mM)	Extratracellular conc. (mM)
Na^+	5-15	145
K^+	140	5
Mg^+	30	1-2
Ca^+	1-2 (10^{-7} is free)	2.5-5
H^+	4×10^{-5} (pH 7.4)	4×10^{-5}
Cl^-	4	110

Eqlbn potentials:

V_{Na} = +50mV to +65mV

V_K = -70mV to –100mV

Resistors embedded in insulating medium

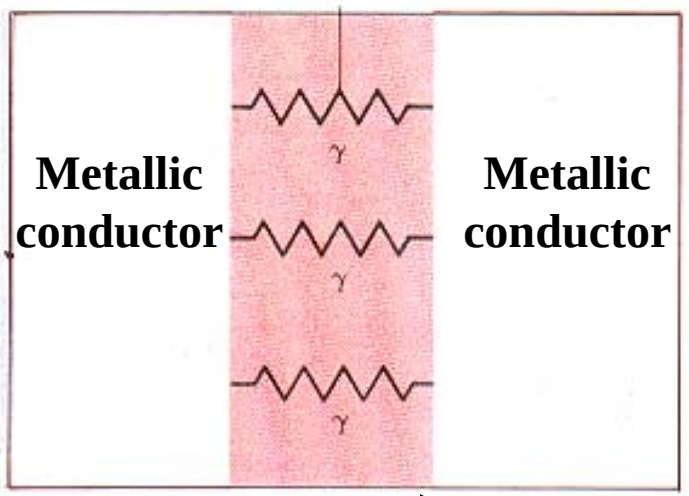

γ = conductance of single resistor

Through parallel resistors:

Total current - $I = (\gamma+\gamma+\gamma)\,V = gV$

g = total conductance

Resistors embedded in insulating medium

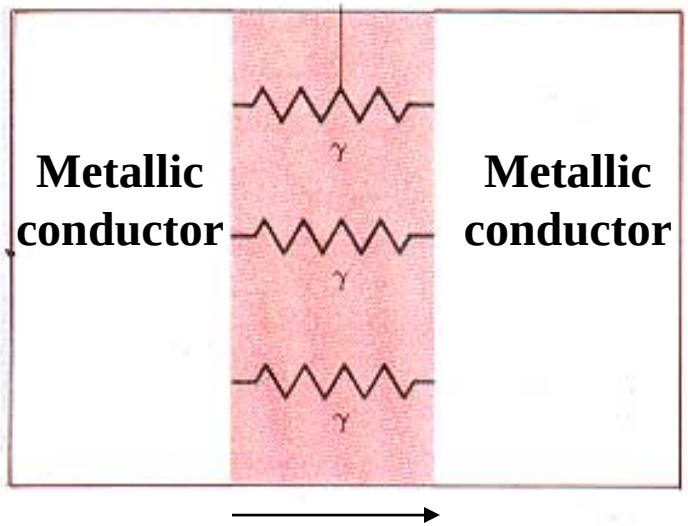

Current = I
Voltage drop = V

Total current - I = (γ+γ+γ) V = gV

γ = conductance of single resistor

g = total conductance

Eqlbn potentials:

V_{na} = +50mV to +65mV

V_K = -70mV to –100mV

Channels embedded in plasma membrane

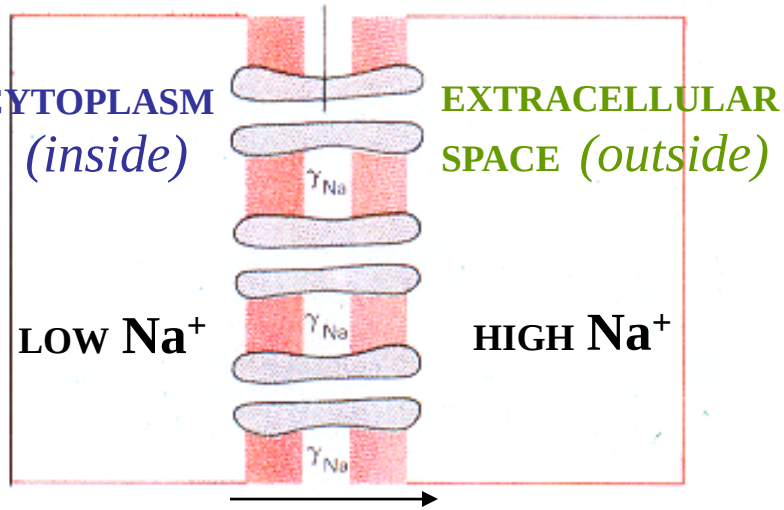

Na^+ current = I_{Na}
Voltage drop = V

Reverse driving force for Na^+ due to conc.diff.
= V_{na}

Net driving force for Na^+ **= $V - V_{Na}$**

Through one channel:
Na^+ current **= I_{Na}[1]** **= $\gamma_{Na}(V - V_{Na})$**

Through 1cm² area of membrane,
total Na^+ current **= I_{Na}** **= $g_{Na}(V - V_{Na})$**

$g_{Na} = \gamma_{Na}$ x no. of channels/cm²

Model for the single beta cell

Bursting electrical activity in the cell is due to the interplay of ionic mechanisms- *Hodgkin & Huxley (1952)*

The channels that are most important to beta cell activity are -

Membrane capacitance

$$C_m \frac{dV}{dt} = -I_{Ca} - I_K - I_{s1} - I_{s2} - I_l$$

Kirchoff's law

$$I_{Ca} = g_{Ca}\ m_\infty(V)\ (V - V_{Ca})$$ **Fast Ca^{2+} current**

$$I_K = g_K\ n\ (V - V_K)$$ **Fast K current**

$$I_{s1} = g_{s1}\ s_1\ (V - V_K)$$ **Slowly inactivating K current**

$$I_{s2} = g_{s2}\ s_2\ (V - V_K)$$ **Very slow inhibitory K current**

$$I_l = g_l\ (V - V_L)$$ **Leakage current**

(Bertram, et al, Biophys. J. 2000; Zimliki, et al, Biophys. J. 2004)

$$\frac{dn}{dt} = \frac{n_\infty(V) - n}{\tau_n(V)}$$
$$\frac{ds_1}{dt} = \frac{s_{1\infty}(V) - s_1}{\tau_{s1}}$$
$$\frac{ds_2}{dt} = \frac{s_{2\infty}(V) - s_2}{\tau_{s2}}$$

$$m_\infty = \frac{1}{1 + exp\left[\frac{(-22-V)}{7.5}\right]}$$
$$n_\infty = \frac{1}{1 + exp\left[\frac{(-9-V)}{10}\right]}$$
$$s_{1\infty} = \frac{1}{1 + exp\left[\frac{(-40-V)}{0.5}\right]}$$
$$s_{2\infty} = \frac{1}{1 + exp\left[\frac{(V_{s2}-V)}{0.4}\right]}$$

Candidates for

s_1 -- K-Ca activation, $I_{K(Ca)}$ inactivation

s_2 -- Ca^{2+} in ER store, ADP ($I_{K(ATP)}$)

n -- gating variable

$$\tau_n = \frac{9.09}{1 + exp\left[\frac{(V+9)}{10}\right]}$$

$\tau_{s1} = 1\text{–}5\ sec$

marginally slow

$\tau_{s2} = 60\text{–}120\ sec$

very slow

PARAMETERS

$g_{s1} = 3\text{–}33\ ps$

$g_{s2} = 32\ ps$

$V_{Ca} = 100\ mV$

$V_K = -80\ mV$

$V_L = -40\ mV$

$V_{s2} = -42\ mV$

$C_m = 4524\ fF$

$g_{Ca} = 280\ ps$

$g_K = 1300\ ps$

$g_l = 25\ ps$

Glucose sensing parameter

DIVERSITY IN SINGLE CELL DYNAMICS

Small heterogeneity in ionic conductances
Different classes of behaviour

gs1 = 33pS

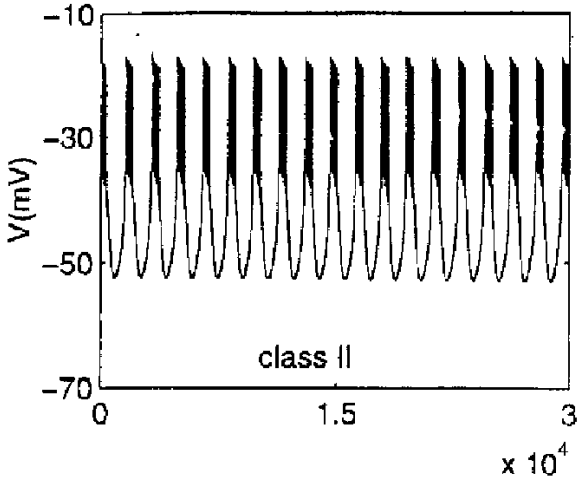

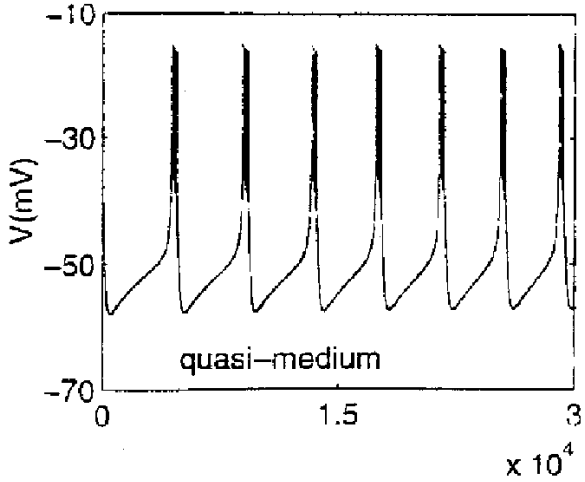

gCa = 300pS
gKATP =15

gK = 1500pS

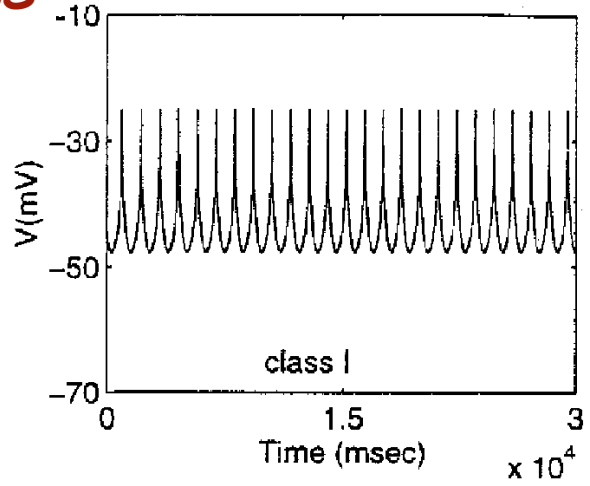

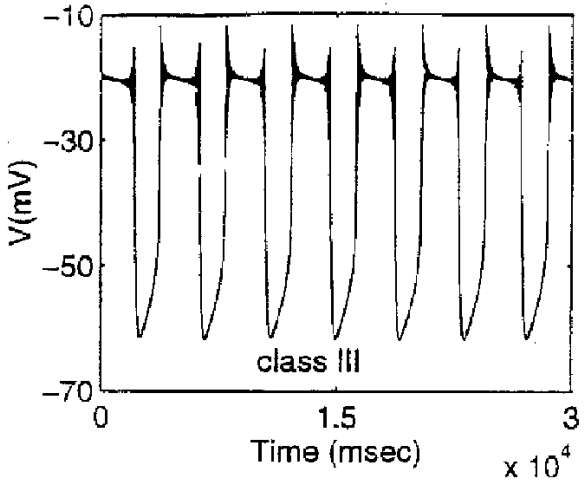

gCa = 325pS

Two cells coupled through gap junction

$$\frac{dV_1}{dt} = -(Iion/Cm) + (gc/Cm)\{V_1 - V_2\} \qquad \frac{dV_2}{dt} = -(Iion/Cm) + (gc/Cm)\{V_2 - V_1\}$$

V_1 and V_2 are voltages of Cell 1 and Cell2

gs1 = 20pS

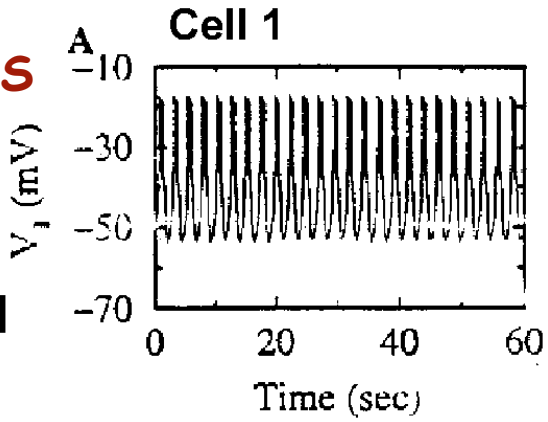

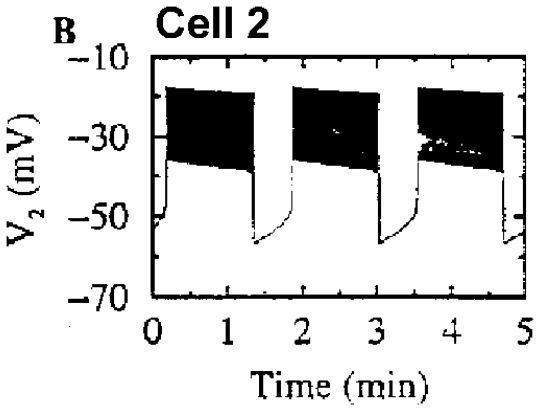

gs1 = 3pS

Uncoupled

Medium bursting through coupling.

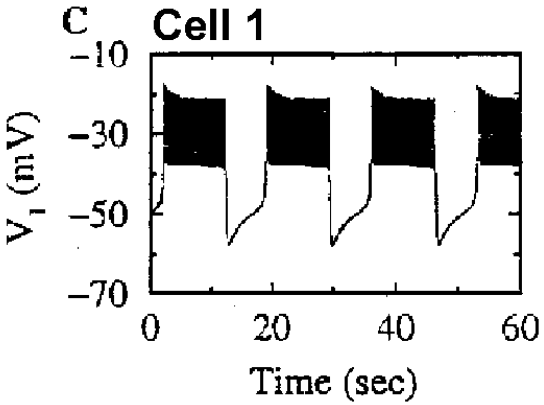

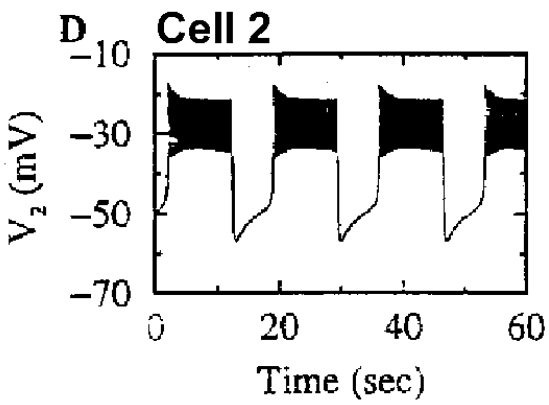

Coupled

No equivalent time constant involved

Gap junctional conductance= gc = 130pS

MODELLING THE ISLET

One dimensional lattice with each Beta Cell coupled to its nearest neighbour through gap junctions

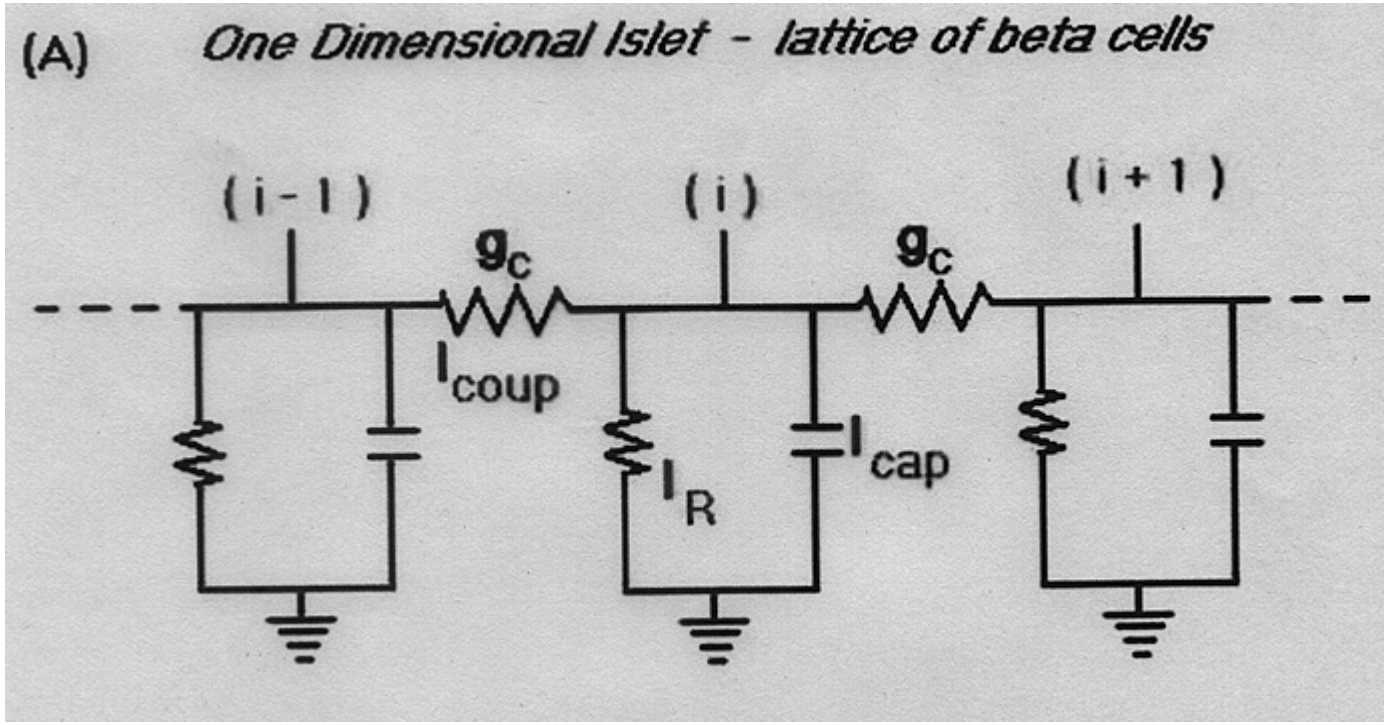

Geometry

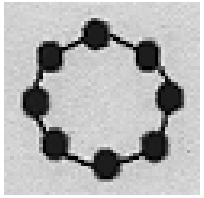

Circular
Periodic boundary

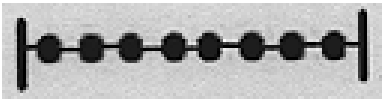

Linear
Fixed boundary

$$\frac{dV_i}{dt} + gmV_i + gc(V_{i+1} - V_i) + gc(V_{i-1} - V_i) = 0$$

Ionic currents (conductances)

Gap junctional conductance

For each cell in the lattice

Assumption of the model:

Cellular interaction in the islet is only electrical - through the gap junction !!!

(Bertram, et al, Biophys. J. 2004)

Types of islets modelled

Lattice size - 5 to 500 cells

Gap junctional coupling strength - 0 to 50,000p

(*Glucose increases gc enormously*)

Homogeneous lattice - all cells have same parameters, but can have different coupling

Study lattice dynamics as a function of

coupling strength (gc), cellular parameters, and their spatial distribution

Heterogenous Lattices

- Randomly distributed burst parameters (gs1, Vs2, gc)
- Patterned distribution of burst parameters (all combinations)

Four type of bursting cells, silent cells taken in different proportions

LINEAR LATTICE - GRADED gs1 (20pS - 2pS)

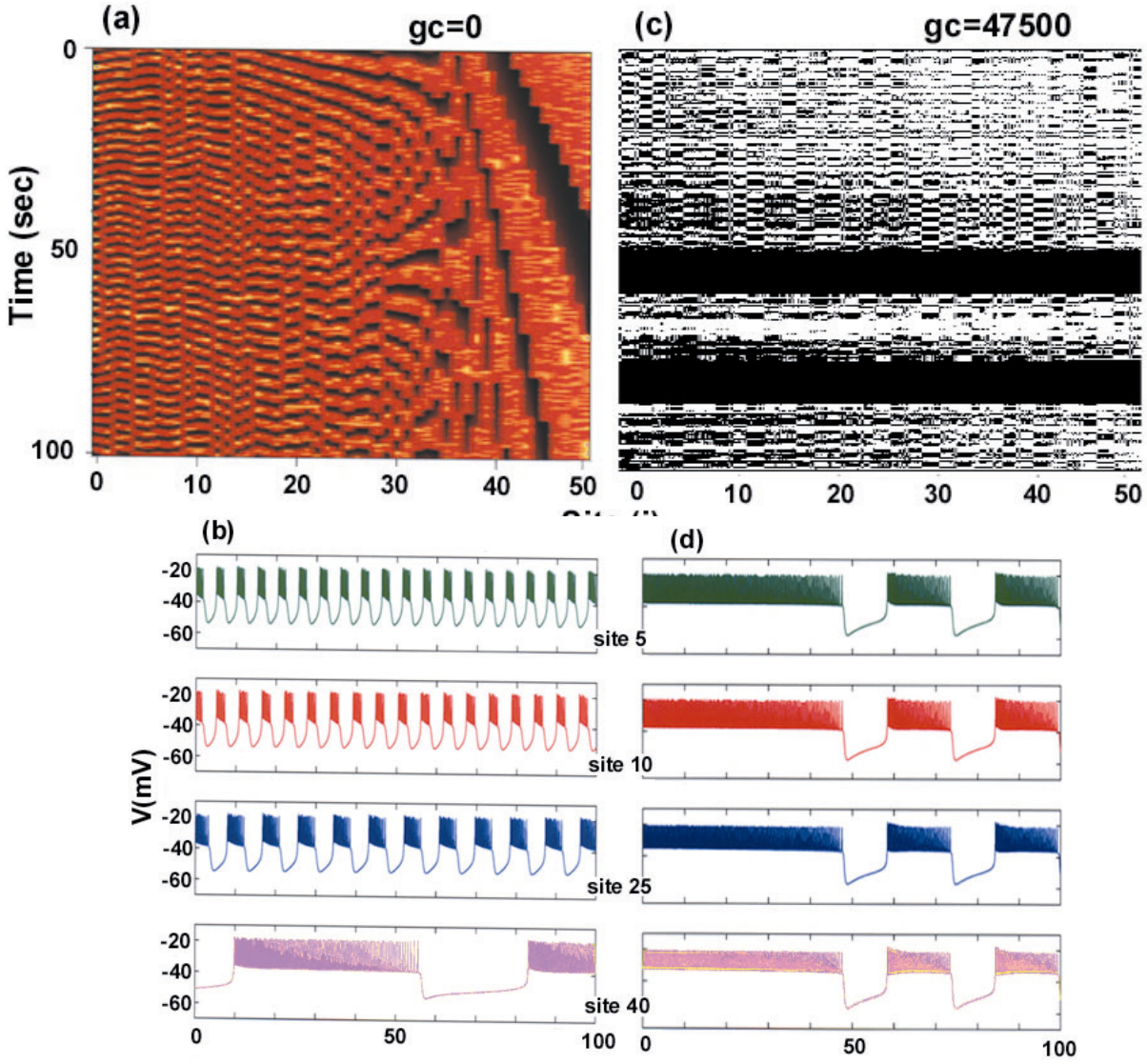

Beautiful synchronised bursts with medium frequency (~25s time period)

Very high gc !!

Gradient in gap junctional coupling strength gc & gs1

Loose to tight coupling

(6000< gc <12000 pS)
-42< Vs_2 <-52

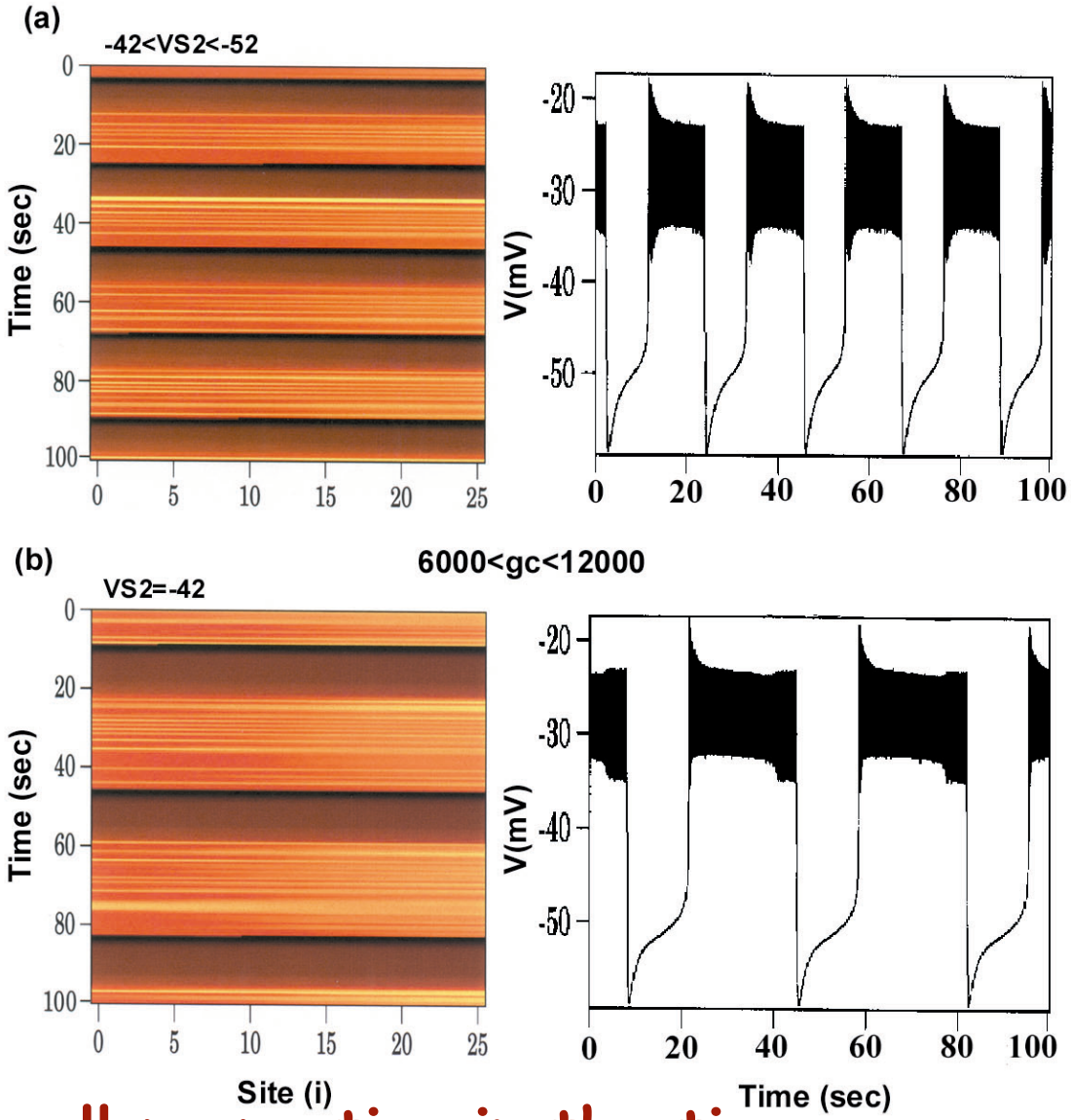

Well-synchronised bursts of medium Frequency (~25 sec)

(6000< gc <12000 pS)

Distribution of cell properties in the tissue controls function

Summary

- Differences in ionic conductances can lead to different burst/oscillation patterns
- The islet cells may have heterogeneity in cellular properties but coupling can lead to synchronised behaviour
- Islet architecture (specific distribution of cell properties in the islet), which may be developmentally regulated, lead to normal function
- There is a dynamic relation between the cell property distribution and burst frequency that may underlie the variation in burst frequencies with concentration of external signals.

Islets can show faster or slower activity in response to glucose, hormones, amino acids, etc.